

AGE AND GROWTH OF THE ARCHEAN KONGLING TERRAIN, SOUTH CHINA, WITH EMPHASIS ON 3.3 GA GRANITOID GNEISSES

SHAN GAO^{*,†}, JIE YANG^{*,§}, LIAN ZHOU^{*}, MING LI^{*}, ZHAOCHU HU^{*},
JINGLIANG GUO^{*,§}, HONGLIN YUAN^{**}, HUJUN GONG^{**}, GAOQIANG XIAO^{*,§},
and JUNQI WEI^{**}

ABSTRACT. The North China craton and the Yangtze craton (South China) both contain Archean rocks in eastern China. Unlike the North China craton, where Archean rocks are widespread, in the Yangtze craton the exposed Archean rocks are only known in the Kongling terrain (360 km²). Zircon U-Pb ages and Lu-Hf isotopic compositions of three granodioritic-trondhjemitic gneisses and three metasedimentary rocks from the Kongling terrain were analyzed by LA-ICP-MS and LA-MC-ICP-MS. Igneous zircons in one trondhjemitic gneiss in the north of the Kongling terrain have an age of 3302 ± 7 (1σ) Ma. Evidence from cathodoluminescence imaging, variations in Th/U and degree of U-Pb age discordance suggest that apparently younger zircons in the same population are variably disturbed 3302 Ma grains. Thus, this trondhjemitic gneiss is the oldest known rock in South China and predates the earlier reported ~2900 Ma granitoid magmatism by 400 Ma. Zircon cores from one granodioritic gneiss in the north of the Kongling terrain also give a concordant age group at 3200 to 3300 Ma. Regardless as inherited or not, these cores crystallized from a magma indistinguishable in age with the trondhjemitic. Concordant U-Pb ages for igneous zircons in one granodioritic gneiss in the south of the Kongling terrain yielded a weighted average ²⁰⁶Pb/²⁰⁷Pb age of 2981 ± 13 Ma (2σ, MSWD=9.7, n=21). The zircon age and initial Hf isotopic compositions are similar to those of widespread granitoid gneisses from the north of the Kongling terrain (2903-2947 Ma), and indicate that the south and north of the Kongling terrain are correlative. The results also reinforce that magmatism of the whole Kongling terrain mainly occurred at 2900 Ma.

Available Hf isotopic data from the Kongling terrain show that juvenile crustal additions occurred mainly between 3150 and 3800 Ma with a significant peak at 3300 to 3500 Ma. The ~3300 Ma zircons from the trondhjemitic gneiss have Hf crust formation ages of 3450 to 3730 Ma, some of which have nearly chondritic ε_{Hf} (t). The whole-rock depleted mantle Nd model age of this rock is 3400 Ma, close to its age of magmatism and consistent with the Hf model age. Its ε_{Nd} value at 3300 Ma is nearly chondritic (1.26). These lines of evidence suggest that the 3300 Ma trondhjemitic represent juvenile crust additions to the pre-existing continental crust.

Key words: Archean, TTG, crustal growth, Yangtze craton, South China

INTRODUCTION

Studies of ancient rocks are critical for understanding formation and evolution of the Early Earth. Granitoids are products of crust formation and evolution (Condie, 1998, 2000; Hawkesworth and Kemp, 2006a, 2006b; Condie and others, 2009). Detrital zircons are a powerful tool to study crustal growth (Condie and others, 2005, 2009; Izuka and others, 2005; Hawkesworth and Kemp, 2006a, 2006b; Liu and others, 2008; Yang and others, 2009). The North China craton and Yangtze craton (South China) are the two largest Archean-bearing blocks in eastern China. They collided along the

* State Key Laboratory of Geological Processes and Mineral Resources, China University of Geosciences, Wuhan 430074, China

** State Key Laboratory of Continental Dynamics, Department of Geology, Northwest University, Xi'an 710069, China

§ Department of Earth Sciences, University of Oxford, South Parks Road, Oxford, OX1 3AN, United Kingdom

† Corresponding author: Telephone: +86 27 67884940; Fax: +86 27 67885096; E-mail address: sgao@263.net (Shan Gao)

Qinling-Dabie-Sulu orogenic belt in the Triassic (for example, Hacker and others, 1998; Ayers and others, 2002; Zheng and others, 2003). Unlike the North China craton, where Archean rocks are widespread, Precambrian basement of the Yangtze craton is exposed sporadically due to coverage by thick Neoproterozoic and Phanerozoic sedimentary sequences. Although increasing evidence shows that Archean (2.5–3.8 Ga) rocks and inherited zircons are present in the Yangtze craton (Gao and others, 1999; Qiu and others, 2000; Liu and others, 2006, 2008; Zhang and others, 2006a, 2006b, 2006c; Zheng and others, 2006), exposed Archean rocks are only known in the Kongling terrain (Gao and Zhang, 1990; Gao and others, 1999; Qiu and others, 2000; Zhang and others, 2006b, 2006c; Jiao and others, 2009) (fig. 1). For the northern segment of this terrain, ion microprobe (SHRIMP) and laser ablation-inductively coupled plasma-mass spectrometry (LA-ICP-MS) U-Pb zircon analyses reveal dominant dioritic-tonalitic-trondhjemitic-granodioritic (DTTG) magmatism at 2.90 to 2.95 Ga and that inherited zircons of 3.0 to 3.2 Ga as xenocrysts were found in the DTTG gneisses (Qiu and others, 2000; Zhang and others, 2006b). Granitoid gneiss of 3218 ± 13 Ma (2σ) in age was also locally identified at the Kongling village (Jiao and others, 2009). Detrital zircons from the metapelites are 2.87 to 3.28 Ga old (Qiu and others, 2000), and the rocks have Nd depleted mantle model ages of 3.07 to 3.21 Ga (Gao and others, 1999). Based on Hf model ages of zircons from the DTTG gneisses, Zhang and others (2006b) imply the presence of ≥ 3.5 Ga continental crust in the Yangtze craton. 3.0 to 3.8 Ga detrital zircons are also present in Neoproterozoic sandstones and tillites from the Yangtze Gorges area (Liu and others, 2006, 2008; Zhang and others, 2006c). However, the sources for the >3.2 Ga inherited and detrital zircons are unknown. In addition, the Kongling terrain consists of northern and southern segments and all previous geochronological studies are confined to the western part of its northern segment. It has been unknown whether the southern segment is Archean and correlative with the northern segment.

Here we report our finding of 3.3 Ga granitoid gneisses from the eastern part of the northern Kongling segment, which are currently the oldest known rocks in South China. We also report the first age dates of granodioritic gneiss and metasedimentary rocks from the southern Kongling segment. The results show that the two Kongling segments are correlative.

GEOLOGICAL SETTING AND SAMPLES

The study area is located in the Yangtze Gorges area (fig. 1). The area is an oval dome structure consisting of the Kongling high-grade metamorphic terrain and the Huangling intrusive complex in the center, which are surrounded by the Neoproterozoic and Phanerozoic sedimentary rocks. The Kongling terrain represents the only known Archean rocks exposed in the Yangtze craton and consists of northern and southern segments (referred to as the North Kongling terrain and South Kongling terrain hereafter), which are separated by the Neoproterozoic Huangling intrusive complex (fig. 1). The dominant North Kongling terrain consists of three types of rock associations (Gao and Zhang, 1990; Gao and others, 1999): (1) dioritic, tonalitic, trondhjemitic, granitic and migmitic gneisses of intrusive origin; (2) metasedimentary rocks; and (3) amphibolite and locally preserved mafic granulite, commonly occurring as lenses, boudins, and layers in the gneisses. These rocks were intruded by the K-feldspar-rich Quanqitang granite and mafic dikes (fig. 1), which yielded U-Pb zircon ages of 1854 ± 17 Ma (2σ) (Xiong and others, 2009) and 1852 ± 11 Ma (2σ) (Peng and others, 2009), respectively. No age and geochemical studies have previously been reported for the South Kongling terrain.

The Huangling intrusive complex is dominated by tonalite-trondhjemitic-granodiorite with minor K-feldspar granite and consists of four suites: Huanglingmiaotronghjemitic, Dalaoling granodiorite, Shandouping tonalite and Xiaofeng tonalite (S.

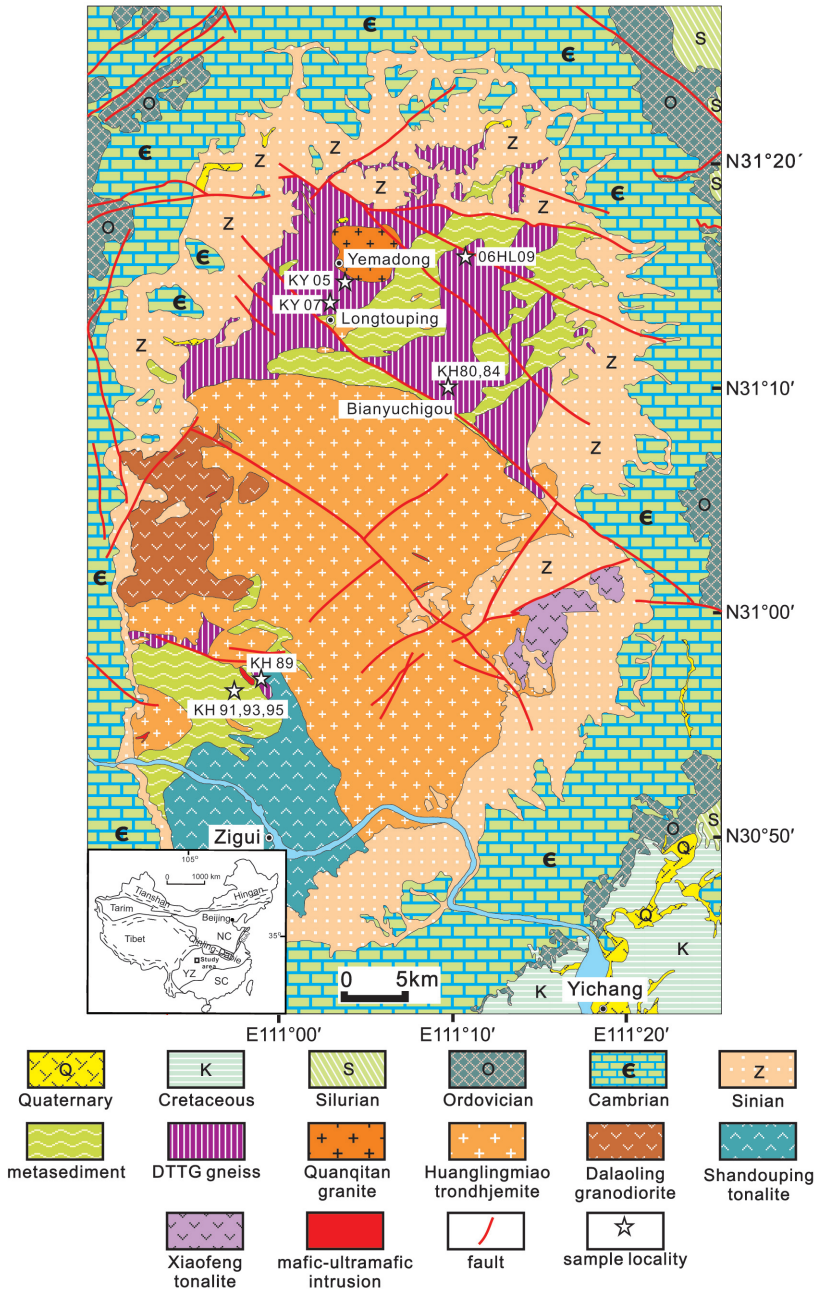


Fig. 1. Geological map of the Archean Kongling terrain. Inset shows major tectonic divisions of China, where YZ and SC denote the Yangtze Craton and South China Orogen, respectively.

Gao, unpublished data) (fig. 1). The Huanglingmiao trondhjemite was dated at 819 ± 7 Ma by SHRIMP zircon U-Pb method (Ma and others, 1984). LA-ICP-MS zircon U-Pb dating yields ages of 795 ± 7 Ma, 794 ± 7 Ma and 744 ± 22 Ma for the Dalaoling

granodiorite, Shandouping and Xiaofeng tonalites, respectively (Ling and others, 2006).

Liu and others (2006, 2008) determined U-Pb age and Hf isotopic compositions of 1130 detrital zircons from 8 sandstone and tillite samples of Neoproterozoic formations from the Yangtze Gorges area. The results reveal four major age groups of 720 to 910 Ma, 1.90 to 2.05 Ga, 2.40 to 2.55 Ga and 2.60 to 2.70 Ga with few grains of 3.2 to 3.5 Ga. Zhang and others (2006a) obtained ages of detrital zircons from one Neoproterozoic sandstone as old as 3.8 Ga. Existing Hf isotopic compositions of detrital zircons from the Neoproterozoic sediments show both juvenile crustal growth and reworking of old crust for all the age groups (Liu and others, 2008). The Paleoproterozoic was a period of prominent crustal reworking whose rock display negative $\epsilon_{\text{Hf}}(t)$ values. The Neoproterozoic was a period of significant juvenile crustal additions, accounting for 68 percent of zircons with positive $\epsilon_{\text{Hf}}(t)$ values similar to those of the depleted mantle. Crustal additions at 3.2 to 3.8 Ga are also significant, as indicated by the zircon Hf continental model ages (see below for discussion).

In order to further investigate the age and growth of the Kongling terrain, particularly the undated parts, we took two granitoid gneisses (KH80, KH84) from the eastern part of the North Kongling terrain and one granodioritic gneiss (KH89) and three metasedimentary samples (KH91, KH93, KH95) from the South Kongling terrain (fig. 1). The former two samples were taken from Bianyuchigou, which is 16 km southeast of the 2.9 Ga trondhjemitic gneiss samples (KY05, KY17) and 14 km south of the 3.2 Ga granitoid gneiss (06HL09) dated by Qiu and others (2000) and Jiao and others (2009), respectively (fig. 1). For samples from the South Kongling terrain, granodioritic gneiss KH89 was taken from Dengcun, while the two metasandstones (KH91, KH95) and one metapelite (KH93) were collected from Maoyacun. All these samples were subjected to amphibolite-facies metamorphism.

Sample KH80 was taken from a large heterogeneous outcrop in a stream, which is dominated by gray gneiss cut by migmitic K-feldspar-rich veins and quartzo-feldspathic pods (left corner of fig. 2A), indicative of later partial melting. However, the taken granodioritic gneiss is free from obvious migmitic veins and comprises 30 percent quartz, 40 percent plagioclase, 20 percent orthoclase and 10 percent biotite (fig. 2D).

Sample KH84 was taken from a relatively homogeneous outcrop of gray gneiss which shows clear alternating dark biotite-rich bands and light quartzspathic bands (fig. 2B). This sample is trondhjemitic gneiss, and comprises 20 percent quartz, 55 percent plagioclase, 10 percent orthoclase and 15 percent biotite (fig. 2E).

For samples from the South Kongling terrain, granodioritic gneiss KH89 was taken from a major road cut (fig. 2C). The rock is relatively homogeneous and foliated and consists of 30 percent quartz, 40 percent plagioclase, 20 percent orthoclase and 10 percent biotite (fig. 2F). The three homogeneous metasedimentary rocks were taken from a small road within a distance of 150 m. No later veins were visible on the outcrops of these three samples (figs. 2G, 2H, 2I). Of them KH91 and KH95 are sandstone and consist of 35 to 40 percent quartz, 30 percent plagioclase, 25 to 30 percent orthoclase, and 5 percent biotite (figs. 2J and 2K). KH93 is graphite- and biotite-bearing paragneiss and consists of 20 percent quartz, 20 percent plagioclase, 25 percent orthoclase, 25 percent biotite and 10 percent sillimanite (fig. 2L).

ANALYTICAL METHODS

Sample Preparation

Whole rock samples were crushed in an alumina disk mill and powdered in an agate mortar.

Zircons were separated by heavy-liquid and magnetic methods and then purified by hand picking under a binocular microscope. >2000 zircon grains were separated,

from which >200 zircon grains were selected and mounted on a double-sided tape, cast in epoxy resin and polished to expose surfaces suitable for LA-ICP-MS analysis. The surfaces of the grain mounts were acid-washed in dilute HNO₃ and pure ethanol to suppress lead contamination.

Major and Trace Element Compositions

Chemical compositions of whole rocks were measured at the State Key Laboratory of Continental Dynamics, Northwest University, China. Major element compositions were analyzed by XRF (Rikagu RIX 2100) using fused glass disks. Trace element compositions were analyzed by ICP-MS (Agilent 7500a with shielded torch) after acid digestion of samples in high-pressure Teflon bombs. Analyses of US Geological Survey basalt and andesite standards (BCR-2, BHVO-1 and AGV-1) indicate precision and accuracy better than 5 percent for major elements and 10 percent for trace and rare earth elements (Rudnick and others, 2004).

Sr-Nd Isotopes

Full details of the Rb-Sr and Sm-Nd procedures were reported in Gao and others (2004). Isotopic ratios were analyzed on a Triton TI mass spectrometer (Thermo Finnigan, Germany) operated in static mode at the State Key Laboratory of Geological Processes and Mineral Resources, China University of Geosciences, Wuhan. ⁸⁷Rb/⁸⁶Sr and ¹⁴⁷Sm/¹⁴⁴Nd ratios were calculated from measured Rb, Sr, Sm and Nd contents determined by ICP-MS. The measured ¹⁴³Nd/¹⁴⁴Nd and ⁸⁷Sr/⁸⁶Sr ratios were normalized to ¹⁴⁶Nd/¹⁴⁴Nd = 0.7219 and ⁸⁶Sr/⁸⁸Sr = 0.1194, respectively. The La Jolla standard measured during the course of our analyses yielded ¹⁴³Nd/¹⁴⁴Nd of 0.511847 ± 1 (2σ_m, n = 2), and BCR-2 yielded ¹⁴³Nd/¹⁴⁴Nd = 0.512612 ± 1 (2σ_m, n = 1). NBS-987 yielded ⁸⁷Sr/⁸⁶Sr = 0.710278 ± 3 (2σ_m, n = 1).

CL Imaging

Prior to *in situ* U-Pb and Hf isotopic analysis, cathodoluminescence (CL) images of zircons were carried out using a Quanta 400 FEG High Resolution Emission Field Environmental Scanning Electron Microscope connected to an Oxford INCA350 energy dispersive system (EDS) and a Gatan Mono CL3+ cathodoluminescence (CL) system at the State Key Laboratory of Continental Dynamics, Northwest University. The imaging conditions were 10 kv with a spot size of 6.7 nm and a working distance of 8.4 mm. The CL images were used to demonstrate the internal textures of zircons and to select optimum spot locations for U-Pb dating.

U-Pb Dating

Zircons were dated in two modes. For KH80 and KH84, zircons were dated *in-situ* using an excimer (193 nm wave length) laser ablation inductively coupled plasma mass spectrometer (LA-ICP-MS) at the State Key Laboratory of Geological Processes and Mineral Resources, Wuhan, China. The ICP-MS used is an Agilent 7500a from Agilent (Japan). The GeoLas 2005 laser-ablation system (MicroLas™ Beam Delivery Systems, Lambda Physik AG, Germany) was used for the laser ablation. Helium was used as carrier gas to provide efficient aerosol transport to the ICP and minimize aerosol deposition around the ablation site and within the transport tube (Eggins and others, 1998; Jackson and others, 2004). The spot size and laser frequency were 30 μm and 10 Hz, respectively. U, Th and Pb concentrations were calibrated by using ²⁹Si as an internal standard and NIST SRM 610 as the reference standard. High-purity argon was used together with an in house helium filtrating column, which resulted in ²⁰⁴Pb and ²⁰²Hg being less than 100 cps in the gas blank. Therefore, the contribution of ²⁰⁴Hg to ²⁰⁴Pb was negligible and no correction was made. ²⁰⁷Pb/²⁰⁶Pb, ²⁰⁶Pb/²³⁸U, ²⁰⁷Pb/²³⁵U and ²⁰⁸Pb/²³²Th ratios, calculated using GLITTER 4.0 (Macquarie University), were

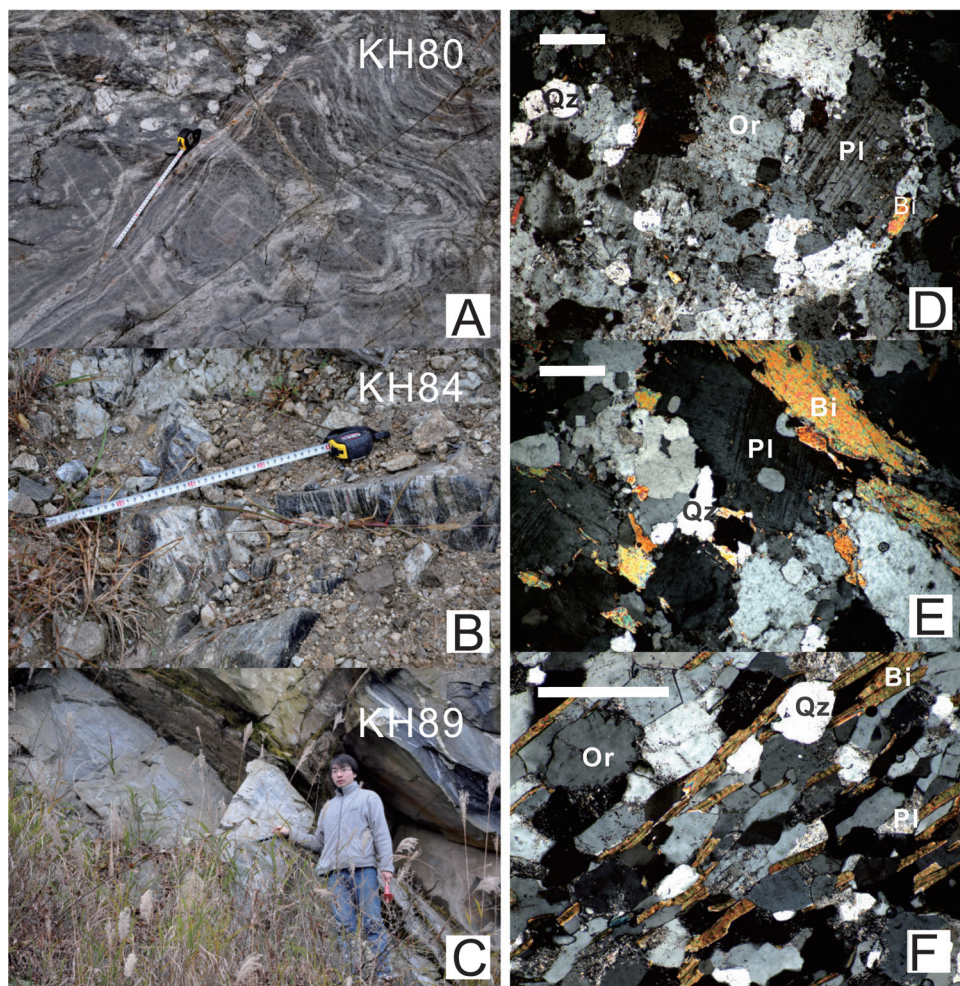


Fig. 2a. Left panel. Photos of field occurrences of samples KH80 (A), KH84 (B), KH89 (C). Rulers are 30 and 40 cm in (a) and (b). Right panel. Corresponding micrographs under cross polarized light of samples KH80 (D), KH84 (E), and KH89 (F).

corrected for both instrumental mass bias and depth-dependent elemental and isotopic fractionation using Harvard zircon 91500 (Wiedenbeck and others, 1995) as external standard. The ages were calculated using ISOPLOT 3 (Ludwig, 2003).

For the other samples, we used our developed technique of simultaneous determinations of U-Pb age, Hf isotopes and trace element compositions of zircon by combining excimer laser ablation quadrupole and multiple collector ICP-MS at the State Key Laboratory of Continental Dynamics, Northwest University (Yuan and others, 2008).

Our measurements of the reference zircon GJ-1 treated as an unknown during the runs of the Kongling zircons yielded weighted $^{206}\text{Pb}/^{238}\text{U}$ ages of 598 ± 3 Ma (2σ , MSWD=2.2, $n=13$), which is in good agreement with the apparent ID-TIMS $^{206}\text{Pb}/^{238}\text{U}$ ages of 598.5 to 602.7 Ma (Jackson and others, 2004). Analytical details for age and trace element determinations of zircons were reported in Yuan and others (2004,

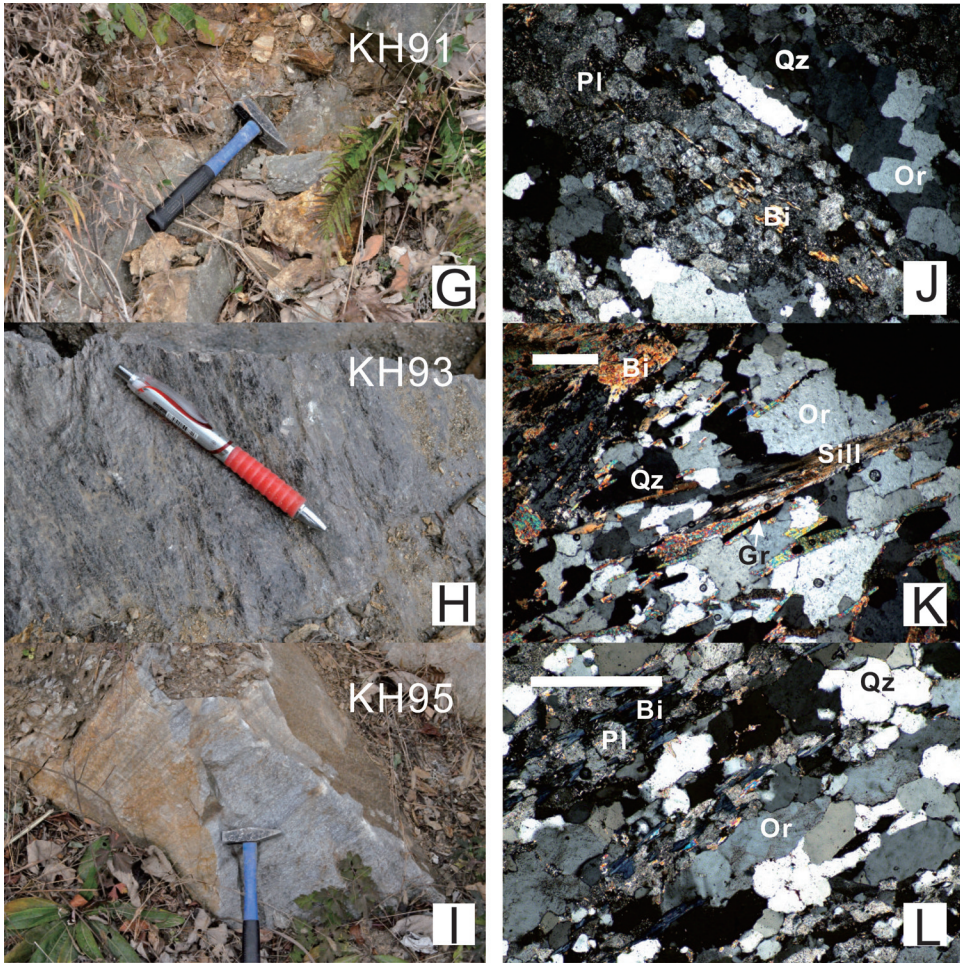


Fig. 2b. Photos of field occurrences of samples KH91 (G), KH93 (H), and KH95 (I). Corresponding micrographs under cross polarized light of samples KH91 (J), KH93 (K), and KH95 (I). Scale bars indicate 0.50 mm. Qz = quartz; Pl = plagioclase; Or = orthoclase; Bi = biotite; Gr = graphite; Sill = sillimanite.

2008). Common Pb corrections were made following the method of Andersen (2002). Because measured ^{204}Pb usually accounts for <0.3 percent of the total Pb, the correction is insignificant in most cases.

As shown by Vermeesch (2004), for provenance studies, a minimum of 117 detrital zircon grains have to be dated from a single sample in order to yield statistically significant results. 101, 143 and 155 zircons were dated for metasediments KH91, KH93 and KH95, respectively.

Hf Isotopes

Hf isotope analysis was done on a Nu Plasma HR MC-ICP-MS (Nu Instruments Ltd., UK), coupled to a GeoLas 2005 excimer ArF laser-ablation system in the State Key Laboratory of Continental Dynamics, Northwest University. The energy density was 15–20 J/cm² and a spot size of 44 μm was used. Helium was also used as carrier gas. We used high-purity argon (99.9995%) and high-purity helium (99.9995%), purified by an

in-house filtration column, which is composed of 15L 13X molecular sieve and can reduce the gas backgrounds of ^{208}Pb and ^{202}Hg to <100 and 400 counts per second (cps) (Yuan and others, 2008). These backgrounds were measured by ion counters (MC-ICP-MS) and correspond to 0.05 and 0.1 ppt, respectively. The sensitivity in laser ablation mode is 7 to 8 volts per 1 percent of hafnium at 44 μm .

Interference correction for Yb and Lu is of paramount importance for precise *in situ* measurements of Hf isotopes in zircon (Woodhead and others, 2004). Interference of ^{176}Lu on ^{176}Hf was corrected by measuring the intensity of the interference-free ^{175}Lu isotope and using the recommended $^{176}\text{Lu}/^{175}\text{Lu}$ ratio of 0.02669 (DeBievre and Taylor, 1993) to calculate $^{176}\text{Lu}/^{177}\text{Hf}$ ratios. Similarly, the interference of ^{176}Yb on ^{176}Hf was corrected by measuring the interference-free ^{172}Yb isotope and using the recommended $^{176}\text{Yb}/^{172}\text{Yb}$ ratio of 0.5886 (Chu and others, 2002) to calculate $^{176}\text{Hf}/^{177}\text{Hf}$ ratios. In doing so, a mean $^{173}\text{Yb}/^{171}\text{Yb}$ ratio for the analyzed spot itself was automatically used in the same run to calculate a mean β_{Yb} value (Iizuka and Hirata, 2005), and then the ^{176}Yb signal intensity was calculated from the ^{173}Yb signal intensity and the mean β_{Yb} value.

According to age dating, the Hf isotopes were measured in two modes. For KH80 and KH84, the analysis was done on the same spots or the same age domains for age determinations, as guided by CL images. For the other samples, we used our developed technique of simultaneous determinations of U-Pb age, Hf isotopes and trace element compositions of zircon by combining excimer laser ablation quadrupole and multiple collector ICP-MS (Yuan and others, 2008). This allows simultaneous collections of data on U-Pb age, Hf isotopes and trace element compositions of the same aerosol from the same spot of zircon. Our measured age and Hf isotope values of six well-characterized zircon standards (91500, Temora-2, GJ-1, Mud Tank, BR266 and Monastery) using this technique agree with the recommended values to within 2σ . Detailed description of the technique and analyses of the six standard zircons were reported in Yuan and others (2008).

RESULTS

Elemental and Sr-Nd Isotopic Compositions

Major and trace element compositions of the six samples under investigation are given in table 1. Granodioritic gneiss KH80 contains 73.6 weight percent SiO_2 , 4.36 weight percent Na_2O and 3.26 weight percent K_2O and a $\text{Na}_2\text{O}/\text{K}_2\text{O}$ ratio of 1.34. Trondhjemitic gneiss KH84 has 70.3 weight percent SiO_2 , 5.54 weight percent Na_2O and 2.05 weight percent K_2O and a $\text{Na}_2\text{O}/\text{K}_2\text{O}$ ratio of 2.70. Both samples show significant heavy rare earth element depletions ($\text{La}_\text{N}/\text{Yb}_\text{N}=26\text{--}36$) (fig. 3A). Sample KH80 is characterized by a remarkable positive Eu anomaly ($\text{Eu}/\text{Eu}^*=5.73$), whereas only a weak negative anomaly is present in KH84 ($\text{Eu}/\text{Eu}^*=0.86$) (fig. 3A). In trace element composition, these two samples are depleted in Nb and Ta and enriched in Pb, characteristic of continental crust and island arc magmas (Rudnick and Gao, 2003) (fig. 3B). KH80 also shows a large positive Sr anomaly (fig. 3B).

For samples from the South Kongling terrain, granodioritic gneiss KH89 has 71.9 weight percent SiO_2 , 3.86 weight percent Na_2O and 3.15 weight percent K_2O and a $\text{Na}_2\text{O}/\text{K}_2\text{O}$ ratio of 1.23. This sample shows the most fractionated REE pattern with $\text{La}_\text{N}/\text{Yb}_\text{N}=92$ and a weak negative Eu anomaly ($\text{Eu}/\text{Eu}^*=0.87$) (fig. 3A). Its trace element composition also shows significant Nb-Ta-Ti depletion and Pb enrichment. Sandstones KH91 and KH95 have 74.1 to 79.2 weight percent SiO_2 . Graphite- and biotite-bearing paragneiss KH93 has 55.5 weight percent SiO_2 and 22.3 weight percent Al_2O_3 . All the three sedimentary rocks are characterized by significant negative Eu

TABLE 1
Chemical and isotopic compositions of rocks from Kongling terrain

	KH80	KH84	KH89	KH91	KH93	KH95
SiO ₂	73.60	70.29	71.85	79.15	55.52	74.11
TiO ₂	0.13	0.29	0.20	0.31	0.83	0.27
Al ₂ O ₃	14.79	15.37	14.85	10.87	21.31	12.12
TFe ₂ O ₃	1.03	2.31	1.98	1.13	8.37	1.81
MnO	0.01	0.03	0.02	<0.01	0.14	0.03
MgO	0.34	0.92	0.57	0.31	4.29	0.60
CaO	1.69	2.21	2.28	0.33	1.38	1.30
Na ₂ O	4.36	5.54	3.86	1.48	1.37	2.68
K ₂ O	3.26	2.05	3.15	5.35	3.71	5.09
P ₂ O ₅	0.02	0.13	0.06	0.04	0.09	0.06
LOI	0.45	0.75	0.81	0.66	2.50	1.46
TOTAL	99.68	99.89	99.63	99.63	99.51	99.53
Li	8.83	18.2	18.6	27.2	80.2	21.0
Be	1.66	2.34	2.66	1.49	1.93	1.60
Sc	1.27	3.58	2.66	3.42	25.7	2.22
V	10.1	23.7	16.4	21.9	178	21.9
Cr	2.49	15.3	3.39	27.8	416	6.95
Co	2.44	5.93	3.86	3.48	42.1	2.22
Ni	2.23	13.7	4.14	10.4	219	3.35
Cu	7.32	13.9	10.2	4.69	70.4	5.49
Zn	24.4	51.4	33.3	21.3	231	35.2
Ga	16.9	20.8	19.9	13.9	27.6	16.0
Ge	0.68	0.91	0.92	0.96	2.88	1.06
Rb	72.1	92.8	147	117	145	126
Sr	331	399	416	57.8	218	202
Y	1.33	9.46	5.24	8.53	27.5	40.1
Zr	88.6	137	199	170	159	233
Nb	2.68	9.30	10.4	9.29	7.51	12.2
Cs	0.54	2.11	3.33	2.06	18.9	1.55
Ba	963	373	787	497	456	1251
La	6.00	25.3	44.9	27.0	38.5	88.0
Ce	9.73	48.9	76.9	52.1	76.4	177
Pr	0.50	5.04	7.86	6.07	9.08	21.7
Nd	2.79	18.4	25.7	21.9	34.4	73.5
Sm	0.50	3.28	3.53	3.68	6.46	12.6
Eu	0.72	0.83	0.85	0.67	1.51	1.91
Gd	0.30	2.67	2.54	2.68	5.89	9.68
Tb	0.05	0.37	0.28	0.37	0.86	1.34
Dy	0.24	1.80	1.13	1.81	4.94	7.44
Ho	0.04	0.33	0.19	0.34	0.99	1.44
Er	0.11	0.81	0.41	0.88	2.63	3.88
Tm	0.02	0.100	0.050	0.12	0.36	0.52
Yb	0.11	0.65	0.33	0.77	2.42	3.26
Lu	0.023	0.088	0.052	0.11	0.35	0.40
Hf	2.56	3.44	5.43	4.70	4.27	6.17
Ta	0.048	0.57	0.95	0.95	0.73	1.27
Pb	22.6	16.7	17.5	12.8	56.5	26.5
Th	0.75	5.73	12.1	10.1	7.51	11.4
U	0.24	0.63	1.10	1.28	2.28	2.35
La _N /Y _N	35.6	26.3	92.3	23.6	10.7	18.2
Eu/Eu*	5.73	0.86	0.87	0.65	0.75	0.53

Major element concentrations are reported in weight percent and trace and rare element concentrations in parts per million (ppm).

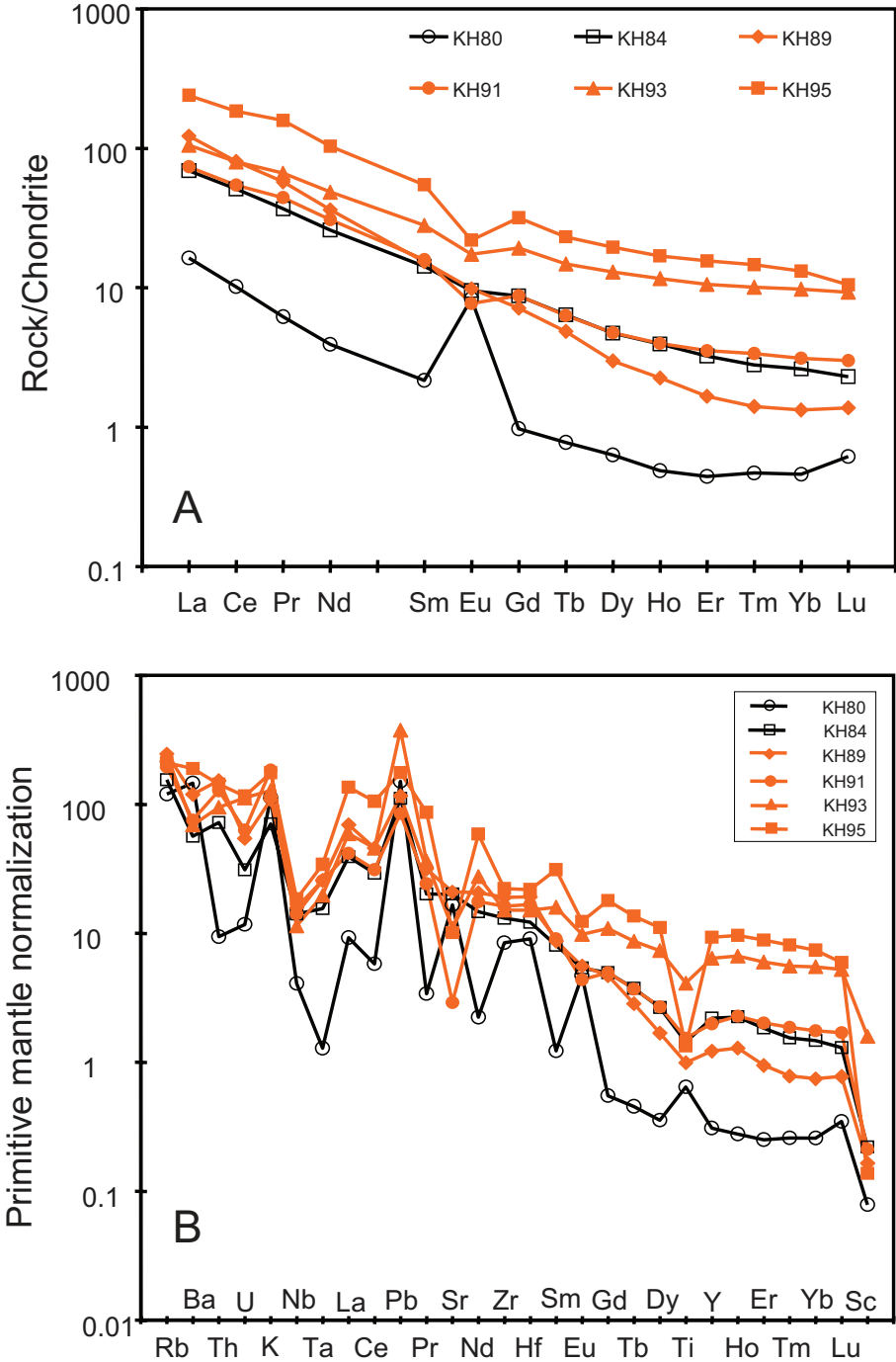


Fig. 3. Chondrite-normalized rare earth element patterns (A) and primitive mantle-normalized trace element distributions (B) of rocks from the Kongling terrain. Open and filled symbols denote samples from the North and South Kongling terrains, respectively. Chondrite and primitive mantle values are taken from Taylor and McLennan (1985) and McDonough and Sun (1995), respectively.

TABLE 2
Sr-Nd isotopic compositions of rocks from Kongling terrain

	KH80	KH80R	KH84	KH89
$^{87}\text{Sr}/^{86}\text{Sr}$	0.730716		0.735792	0.743932
$2\sigma_m$	4		4	3
$^{87}\text{Rb}/^{86}\text{Sr}$	0.63164		0.67476	1.02600
$^{143}\text{Nd}/^{144}\text{Nd}$	0.510710	0.510718	0.510759	0.510369
$2\sigma_m$	6	9	1	2
$^{147}\text{Sm}/^{144}\text{Nd}$	0.10786		0.10773	0.08303
T_{DM} (Ga)	3.48		3.41	3.22
ϵ_{Nd} (0 Ma)	-37.57		-36.61	-44.22
ϵ_{Nd} (2981 Ma)	-3.47		-2.45	-0.56
ϵ_{Nd} (3300 Ma)	0.24		1.26	4.19

The decay constant (λ) of ^{147}Sm used in model age calculation is 0.00654 Ga^{-1} . The model age based on depleted mantle (T_{DM}) assumes a linear evolution of isotopic composition from $\epsilon_{\text{Nd}}(T) = 0$ at 4.56 Ga to approximately +10 at the present time. The notation of ϵ_{Nd} follows DePaolo and Wasserburg (1976), and model ages (T_{DM}) were calculated using equations: $T_{\text{DM}} = 1/\lambda \times \ln\{1 + [({}^{143}\text{Nd}/{}^{144}\text{Nd})_{\text{sample}} \times 0.51315] / [({}^{147}\text{Sm}/{}^{144}\text{Nd})_{\text{sample}} \times 0.2137]\}$.

anomalies ($\text{Eu}/\text{Eu}^* = 0.53\text{--}0.75$) similar to the post-Archean sediments (Taylor and McLennan, 1985; Rudnick and Gao, 2003) (fig. 3A). Their trace element compositions are more or less similar to KH89 with Nb-Ta-Ti depletion and Pb enrichment. However, they all show pronounced Sr depletion (fig. 3B).

Sr-Nd isotopic compositions of the three dated granitoid gneisses are listed in table 2. As will be described below, sample KH84 has magma emplacement age of 3.3 Ga. Sample KH80 may be of the same age or contains inherited materials of the same age. Initial ϵ_{Nd} values of both rocks at 3.3 Ga are 0.24 to 1.26. Sample KH89 was emplaced at 2981 Ma. Its initial ϵ_{Nd} value at the time of emplacement is close to chondritic (-0.56).

Zircon U-Pb Age

U-Pb data for concordant (age concordance within $100 \pm 10\%$) and discordant (age concordance out of $100 \pm 10\%$) zircons are given in Appendix table A1 (<http://earth.geology.yale.edu/~ajs/SupplementaryData/2011/02GaoTableA1.xls>) and table A2 (<http://earth.geology.yale.edu/~ajs/SupplementaryData/2011/03GaoTableA2.xls>), respectively. Our following discussion will be confined to concordant zircons and the $^{206}\text{Pb}/^{207}\text{Pb}$ age will be used, as all of the concordant zircons are older than 1.0 Ga. Errors reported for a single grain/spot analysis are 1σ as presented in Appendix table A1 (<http://earth.geology.yale.edu/~ajs/SupplementaryData/2011/02GaoTableA1.xls>) and Appendix table A2 (<http://earth.geology.yale.edu/~ajs/SupplementaryData/2011/03GaoTableA2.xls>) and 2σ for the weighted average age of a concordant age group.

Eastern Part of North Kongling Terrain

Zircons from KH80 and KH84 are mostly translucent, light yellow and prismatic. Their length ($100 \mu\text{m}$) to width (up to $450 \mu\text{m}$) ratios range from 1.5: 1 to 5:1. Most of them show oscillatory zoning typical of magmatic zircons (figs. 4A, 4F to 4N). Some show a core-rim structure (figs. 4A to 4D). Few magmatic zircons have very thin and bright rims (figs. 4H, 4J, and 4K).

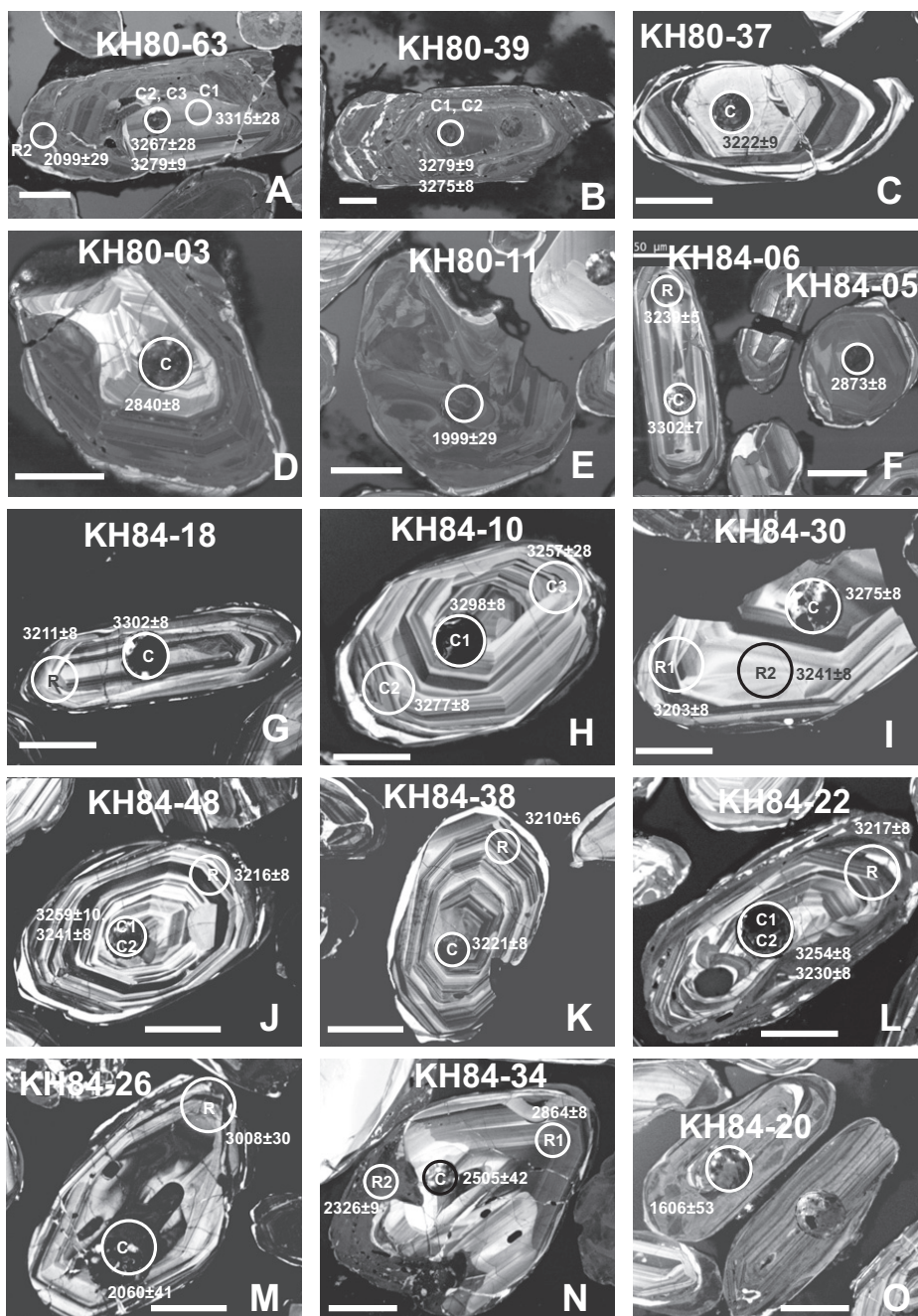


Fig. 4. Cathodoluminescence images of zircons in granodioritic gneiss KH80 (A to E) and trondhjemitic gneiss KH84 (F to O). White bars indicate 50 μm . Note two analyses KH80-63C2 and C3 in (A) were made on the same spot. This is also true for KH80-39C1, C2 in (B), KH84-48C1, C2 in (J) and KH84-22C1, C2 in (L).

Granodioritic Gneiss KH80

Ninety-eight LA-ICP-MS U-Pb dates were obtained on KH80. The concordant ages can be divided into four groups (figs. 5A and 6A; Appendix table A1, <http://earth.geology.yale.edu/~ajs/SupplementaryData/2011/02GaoTableA1.xls>):

(1) 3.1 to 3.3 Ga, which is represented by ten concordant analyses with apparent $^{206}\text{Pb}/^{207}\text{Pb}$ ages ranging from 3101 to 3315 Ma. They yield a weighted average $^{206}\text{Pb}/^{207}\text{Pb}$ age of 3262 ± 27 Ma (2σ , MSWD=8.9, $n=10$). They occur as cores with later overgrowths. The cores are characterized by weak oscillatory zoning (figs. 4A and 4C) or are dark and structureless (fig. 4B). Their Th/U varies between 0.35 and 0.75. In contrast, the overgrowths vary widely in CL image, age and Th/U ratio. They are weakly zoned (KH80-63R2) (fig. 4A), structureless (fig. 4B) or oscillatory (fig. 4C). The oldest grain is KH80-63. Three analyses on its weak oscillatory zoned core give the ages of 3315 ± 28 Ma (KH80-63C1), 3267 ± 28 Ma (KH80-63C2) and 3279 ± 8 Ma (KH80-63C3) (fig. 4A), with Th/U ratios of 0.60 to 0.75. The core is surrounded by later overgrowths (KH80-63R2) of 2099 ± 29 Ma with Th/U of 0.11 and dark zoning. The core of grain KH80-37 (KH80-37C1) gives an age of 3222 ± 9 Ma and Th/U=0.47 (fig. 4C).

(2) 2.7 to 2.8 Ga, which is represented by 15 concordant analyses with apparent $^{206}\text{Pb}/^{207}\text{Pb}$ ages ranging from 2730 to 2844 Ma. They show oscillatory zoning (fig. 4D) and give a weighted average $^{206}\text{Pb}/^{207}\text{Pb}$ age of 2796 ± 16 Ma (2σ , MSWD=10.1, $n=15$). Their Th/U ratios range from 0.20 to 0.53.

(3) 2.5 to 2.6 Ga, which is denoted by 14 concordant analyses with apparent $^{206}\text{Pb}/^{207}\text{Pb}$ ages ranging from 2529 to 2691 Ma. They give a weighted average $^{206}\text{Pb}/^{207}\text{Pb}$ age of 2615 ± 29 Ma (2σ , MSWD=18, $n=14$). Their Th/U ratios range from 0.15 to 0.55. They exhibit oscillatory zoning (not shown).

(4) 1.9 to 2.0 Ga, which is represented by 11 analyses with apparent $^{206}\text{Pb}/^{207}\text{Pb}$ ages ranging from 1916 to 2099 Ma. They give a weighted average $^{206}\text{Pb}/^{207}\text{Pb}$ age of 1981 ± 16 Ma (2σ , MSWD=3.5, $n=11$) and Th/U=0.06 to 0.15. They are typically dark, weakly zoned and structureless in CL images and occur as separate grains or overgrowths (figs. 4A and 4E).

In addition, the 3.2 Ga, 2.6 Ga and 1.9 Ga zircons form trends of Pb loss with a lower intercept at ~ 600 Ma (fig. 5A).

Trondhjemitic Gneiss KH84

Seventy-four U-Pb dates were obtained from KH84 [Appendix table A1 (<http://earth.geology.yale.edu/~ajs/SupplementaryData/2011/02GaoTableA1.xls>) and table A2 (<http://earth.geology.yale.edu/~ajs/SupplementaryData/2011/03GaoTableA2.xls>)]. The concordant ages can be divided into three major groups [figs. 5B and 6B; Appendix table A1 (<http://earth.geology.yale.edu/~ajs/SupplementaryData/2011/02GaoTableA1.xls>)]:

(1) 3.0 to 3.3 Ga, which is represented by 32 analyses with apparent $^{206}\text{Pb}/^{207}\text{Pb}$ ages ranging from 3072 to 3302 Ma. They yield a weighted average $^{206}\text{Pb}/^{207}\text{Pb}$ age of 3234 ± 15 Ma (2σ , MSWD=23, $n=32$). Their Th/U ratios vary between 0.19 and 0.78. Unlike those from KH80, the whole grains of these oldest zircons show homogeneous clear oscillatory zoning except very thin bright rims on some of them and there is no significant core-rim difference in age (figs. 4G to 4L). Of them the oldest grains are KH84-06 and KH84-18. Both give ages of $3302 \pm 7/8$ (figs. 4F and 4G).

(2) 2.8 to 2.9 Ga, which is represented by 18 analyses with apparent $^{206}\text{Pb}/^{207}\text{Pb}$ ages ranging from 2860 to 3011 Ma. They give a weighted average $^{206}\text{Pb}/^{207}\text{Pb}$ age of 2913 ± 18 Ma (2σ , MSWD=15, $n=18$). Their Th/U ratios vary from 0.37 to 1.22. They typically show oscillatory zoning (for example, KH84-26R, KH84-34R1; figs. 4M and 4N) and were altered by later overgrowth. This is well exemplified by KH84-26 with the much younger 2060 Ma black irregular core whose Th/U ratio is extremely low (0.048). The 2.8 Ga portion of KH84-34 was also modified by 2505 Ma oscillatory

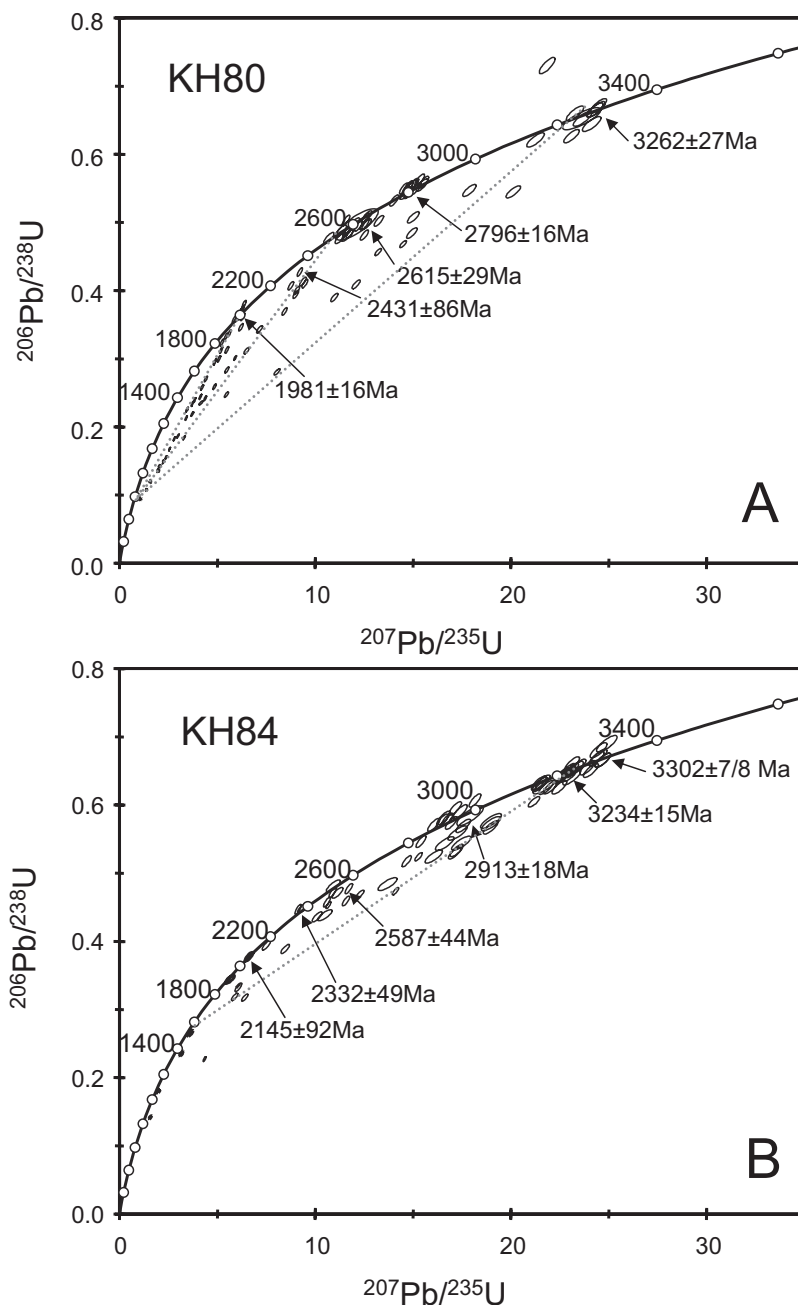


Fig. 5. Zircon U-Pb concordia plots for granodioritic gneiss KH80 (A) and trondhjemitic gneiss KH84 (B) from the North Kongling terrain. Error ellipses are shown at 1σ .

overgrowth in the core and rimmed by the 2326 Ma overgrowth. But structureless grains are also present (KH84-05; 2873 ± 8 Ma, Th/U=0.39) (fig. 4F).

(3) 2.5 to 2.6 Ga, which is denoted by 9 analyses with apparent $^{206}\text{Pb}/^{207}\text{Pb}$ ages ranging from 2505 to 2680 Ma. They give a weighted average $^{206}\text{Pb}/^{207}\text{Pb}$ age of

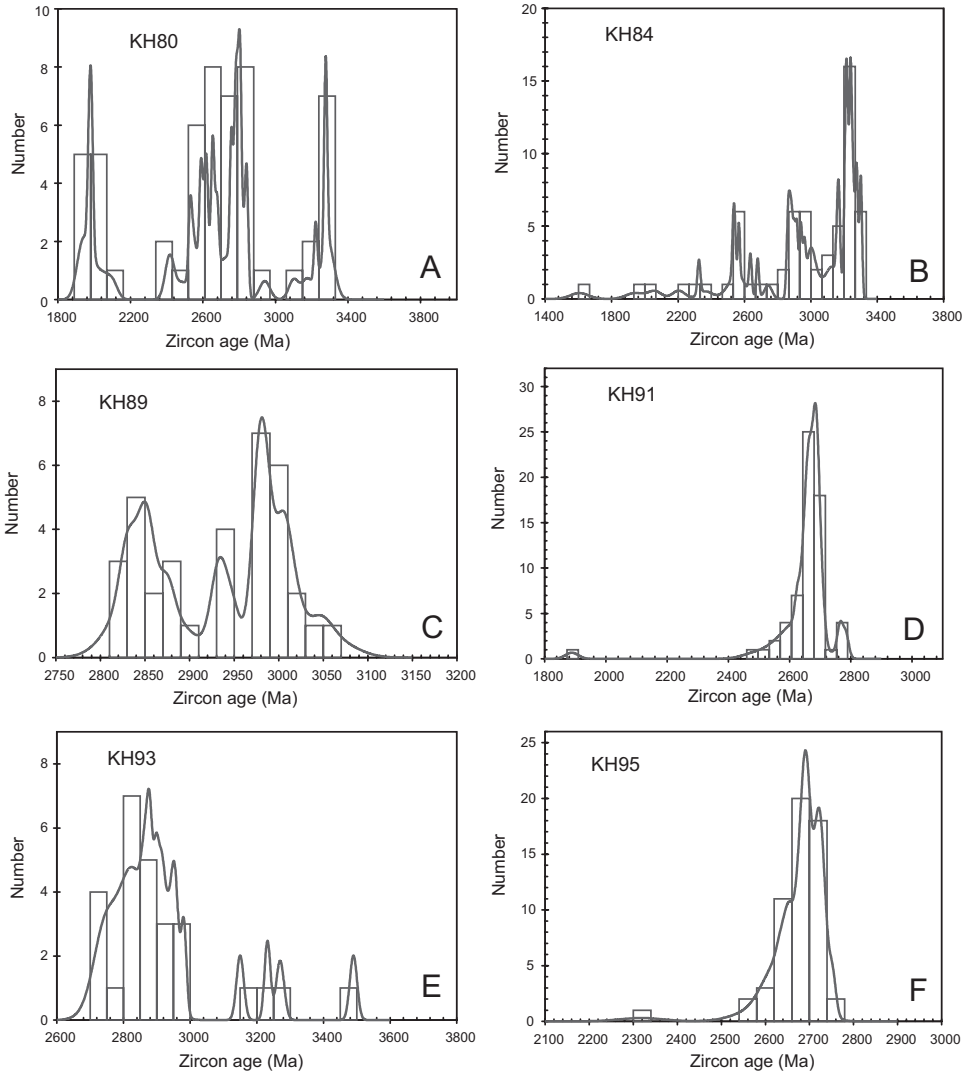


Fig. 6. Probability density plots of concordant zircon $^{206}\text{Pb}/^{207}\text{Pb}$ ages of granodioritic and trondhjemitic gneisses KH80 and KH84 (A, B) from the North Kongling terrain and granodioritic gneiss KH 89 (C) and metasedimentary rocks KH91, KH93 and KH95 (D, E, F) from the South Kongling terrain.

2587 ± 44 Ma (2σ , MSWD=34, $n=9$). Their Th/U ratios range from 0.14 to 0.36. As described above, they typically show oscillatory zoning (for example, KH84-34C; fig. 4N).

There are two minor younger age populations:

(1) 2.3 to 2.4 Ga, which is represented by 4 analyses with apparent $^{206}\text{Pb}/^{207}\text{Pb}$ ages ranging from 2304 to 2434 Ma. They give a weighted average $^{206}\text{Pb}/^{207}\text{Pb}$ age of 2332 ± 49 Ma (2σ , MSWD=3.4, $n=4$). Their Th/U ratios vary from 0.059 to 0.31. They usually occur as dark overgrowths (KH84-34R2; fig. 4N).

(2) 1.9 to 2.1 Ga, which is represented by 6 analyses with apparent $^{206}\text{Pb}/^{207}\text{Pb}$ ages ranging from 1941 to 2212 Ma. They give a weighted average $^{206}\text{Pb}/^{207}\text{Pb}$ age of 2145 ± 92 Ma (2σ , MSWD=5.5, $n=6$). Their Th/U ratios vary from 0.048 to 0.17. They usually also occur as black overgrowths (KH84-26C, fig. 4M).

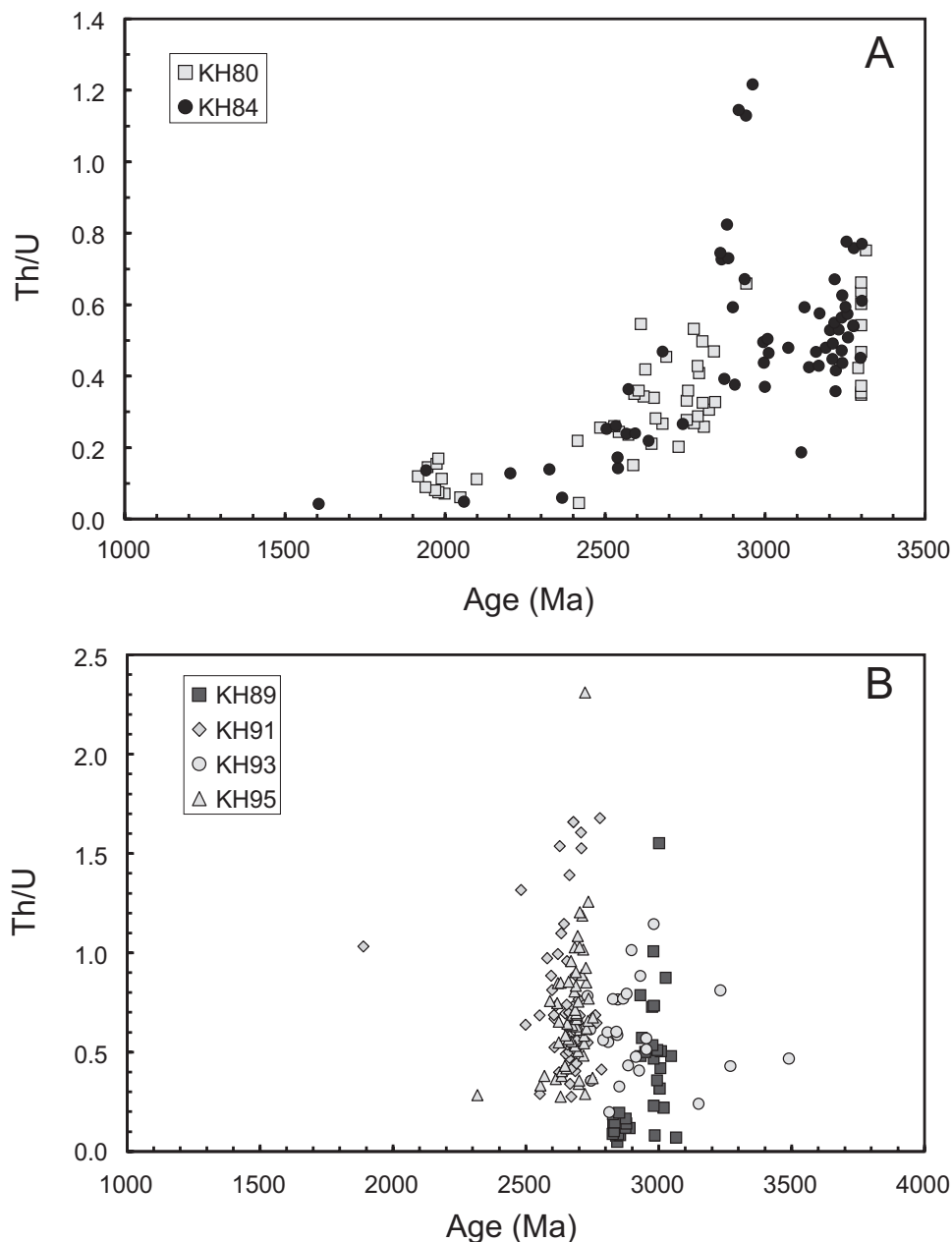


Fig. 7. Variation of concordant zircon Th/U ratio with age for KH80 and KH84 from the North Kongling terrain (A) and for KH89, KH91, KH93 and KH95 (B) from the South Kongling terrain.

One concordant zircon has age of 1606 ± 53 Ma (KH84-20; fig. 4O) and $\text{Th}/\text{U} = 0.042$. Zircon Th/U ratios of the two North Kongling granitoid gneisses show a clear decreasing trend with decreasing age (fig. 7A). The values of all the > 2.8 Ga zircons vary from 0.30 up to 1.2, typical of igneous zircons, whereas < 2.4 Ga zircons have a Th/U ratio that ranges from 0.20 to 0.04, characteristic of metamorphic zircons

(Hoskin and Schaltegger, 2003). Zircons of the intermediate ages (2.4–2.8 Ga) show intermediate Th/U ratios (0.2–0.4).

South Kongling Terrain

Granodioritic gneiss KH89.—Sixty-one analyses were done on granodioritic gneiss KH89 (Appendix table A1, <http://earth.geology.yale.edu/~ajs/SupplementaryData/2011/02GaoTableA1.xls> and Appendix table A2, <http://earth.geology.yale.edu/~ajs/SupplementaryData/2011/03GaoTableA2.xls>). They form a discordia with the upper intercept at 2951 ± 20 Ma and lower intercept at 726 ± 120 Ma (fig. 8A). Twenty-one 2.93 to 3.07 Ga concordant zircons at the upper intercept give a weighted average $^{206}\text{Pb}/^{207}\text{Pb}$ age of 2981 ± 13 Ma (2σ , MSWD=9.7, $n=21$) (fig. 8A). Fourteen 2.8 Ga concordant zircons produce a weighted average $^{206}\text{Pb}/^{207}\text{Pb}$ age of 2849 ± 10 Ma (2σ , MSWD=2.3, $n=14$). All but two ~ 3.0 Ga grains have Th/U ratios of 0.20 to 1.55 (fig. 7B). In contrast, the values of the 2.8 Ga zircons are ≤ 0.20 (fig. 7B). The ~ 3.0 Ga zircons show clear to weak oscillatory zoning or are structureless (figs. 9A, 9B and 9C), while the 2.8 Ga zircons are structureless (figs. 9D and 9E).

Metasediments KH91, KH93 and KH95.—One hundred and one analyses were made on metasandstone KH91 (Appendix table A1, <http://earth.geology.yale.edu/~ajs/SupplementaryData/2011/02GaoTableA1.xls> and table A2 <http://earth.geology.yale.edu/~ajs/SupplementaryData/2011/03GaoTableA2.xls>). Fifty-seven concordant zircons form a group that has a weighted average $^{206}\text{Pb}/^{207}\text{Pb}$ age of 2671 ± 6 Ma (2σ , MSWD=5.4, $n=57$) (fig. 10A). They have Th/U ratios of 0.28–1.66 (fig. 7B). Five older 2733–2785 Ma zircons give a weighted average $^{206}\text{Pb}/^{207}\text{Pb}$ age of 2771 ± 15 Ma (2σ , MSWD=1.5, $n=5$). Their Th/U ratios range from 0.41 to 1.68. There is one concordant zircon (KH91-05) of apparent $^{206}\text{Pb}/^{207}\text{Pb}$ age of 1889 ± 21 (1σ), with a Th/U ratio of 1.03.

One hundred and fifty analyses were carried out on another metasandstone KH95 (Appendix table A1, <http://earth.geology.yale.edu/~ajs/SupplementaryData/2011/02GaoTableA1.xls> and Appendix table A2, <http://earth.geology.yale.edu/~ajs/SupplementaryData/2011/03GaoTableA2.xls>). Fifty-eight concordant zircons form a group yielding a weighted average $^{206}\text{Pb}/^{207}\text{Pb}$ age of 2697 ± 8 (2σ , MSWD=9.3, $n=58$) (fig. 10B). They have Th/U ratios of 0.28 to 2.31 (fig. 7B) with an average of 0.71. There is one concordant zircon (KH95-77) of apparent $^{206}\text{Pb}/^{207}\text{Pb}$ age of 2318 ± 50 (1σ), with a Th/U ratio of 0.28. The zircon ages and characteristics are very similar to those of KH91.

One hundred and forty three analyses were carried out on metapelite KH93 (Appendix table A1, <http://earth.geology.yale.edu/~ajs/SupplementaryData/2011/02GaoTableA1.xls> and table A2 <http://earth.geology.yale.edu/~ajs/SupplementaryData/2011/03GaoTableA2.xls>). Four >3.1 Ga concordant zircons were found in this sample (fig. 8B): KH93-08 has a $^{206}\text{Pb}/^{207}\text{Pb}$ age of 3490 ± 11 Ma (1σ) (Th/U=0.47), KH93-136 3270 ± 12 Ma (Th/U=0.43), KH93-44 3232 ± 9 Ma (Th/U=0.81), and KH93-23 3150 ± 11 Ma (Th/U=0.24). The other twenty-five concordant zircons form a group that gives a weighted average age of 2911 ± 22 Ma (2σ , MSWD=13, $n=25$) (fig. 8B).

Hf Isotopes

Hf isotopes were analyzed on 202 selected close to concordant zircons from the six samples under investigation (Appendix table A1, <http://earth.geology.yale.edu/~ajs/SupplementaryData/2011/02GaoTableA1.xls>). The initial $^{176}\text{Hf}/^{177}\text{Hf}$ ratios were calculated with reference to the chondritic reservoir (CHUR) at the time of zircon growth from magmas. The decay constant for ^{176}Lu and the chondritic ratios of $^{176}\text{Hf}/^{177}\text{Hf}$ and $^{176}\text{Lu}/^{177}\text{Hf}$ used in calculations are $1.865 \times 10^{-11} \text{ yr}^{-1}$ (Scherer and others, 2001) and 0.282772 and 0.0332 (Bichert-Toft and Albarède, 1997), respectively. The single-stage model age (T_{DM1}) was calculated relative to the depleted mantle with a present-day $^{176}\text{Hf}/^{177}\text{Hf} = 0.28325$ and $^{176}\text{Lu}/^{177}\text{Hf} = 0.0384$ (Griffin

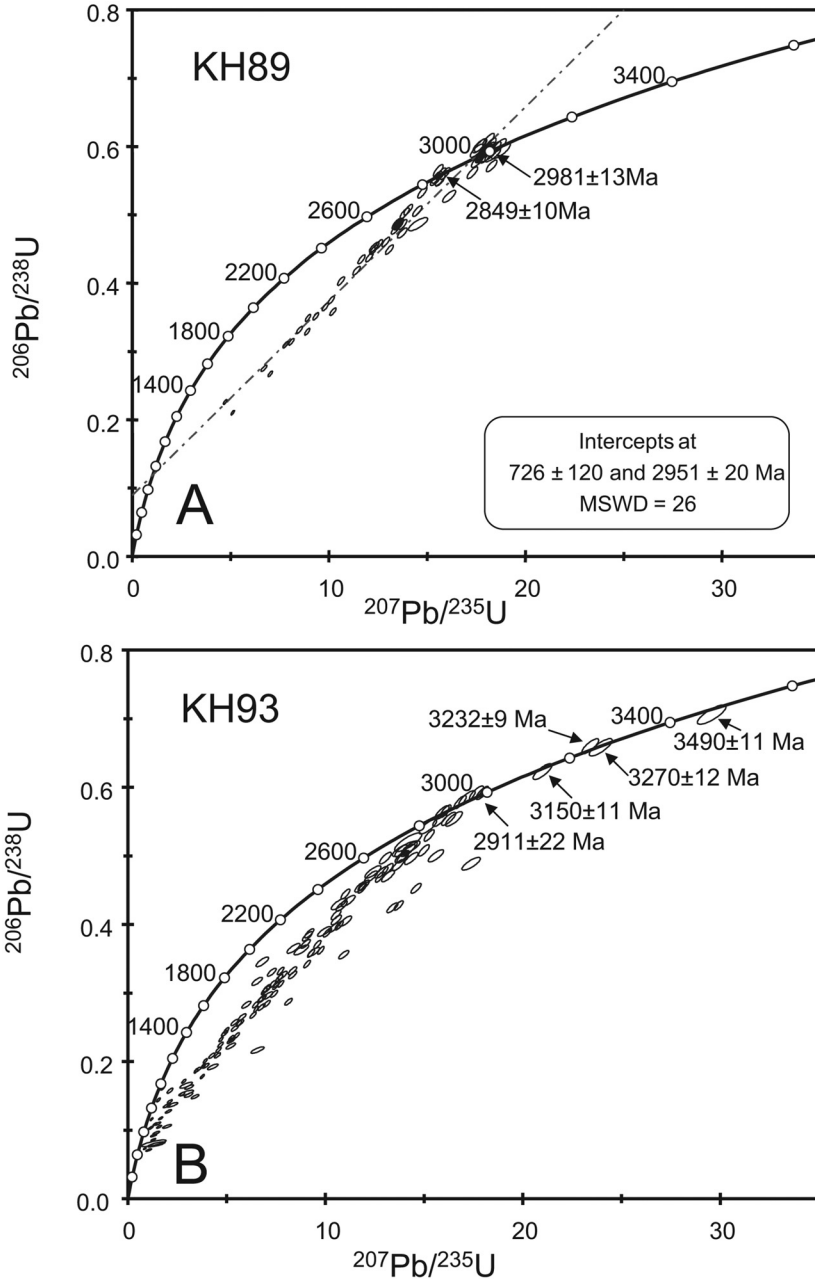


Fig. 8. Zircon U-Pb concordia plots for granodioritic gneiss KH89 (A) and metapelite KH93 (B) from the South Kongling terrain. Error ellipses are shown at 1σ .

and others, 2000). A two-stage continental model age (T_{DM2}) was also calculated by projecting the initial $^{176}\text{Hf}/^{177}\text{Hf}$ of zircon back to the depleted mantle growth curve using $^{176}\text{Lu}/^{177}\text{Hf} = 0.0093$ for the upper continental crust (Vervoort and Patchett, 1996).

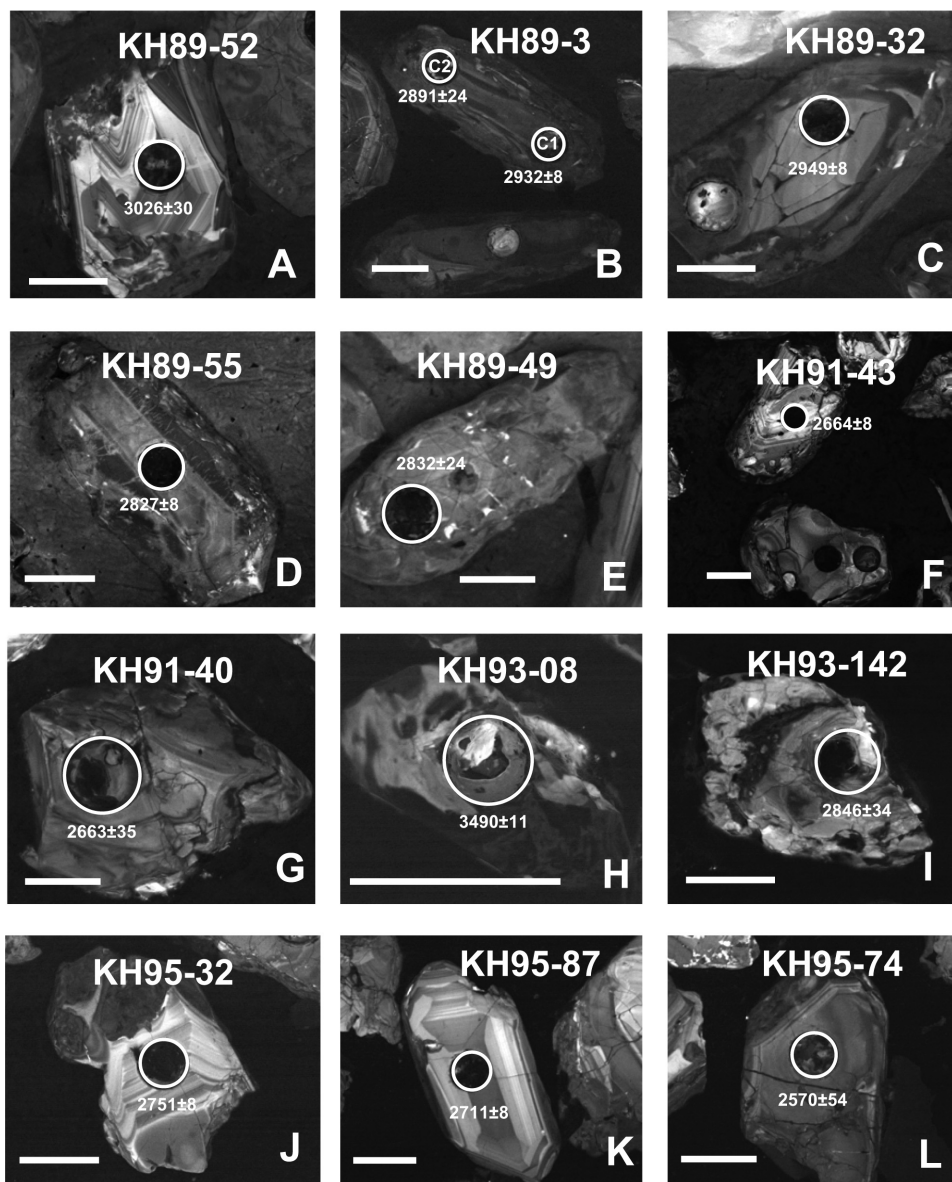


Fig. 9. Cathodoluminescence images of zircons in KH89 (A to E), KH91 (F, G), KH93 (H, I) and KH95 (J to L) from the South Kongling terrain. White bars indicate 50 μm .

Eastern Part of North Kongling Terrain

Hf isotopes were analyzed on 45 closed to concordant zircons for each of KH80 and KH84 (Appendix table A1, <http://earth.geology.yale.edu/~ajs/SupplementaryData/2011/02GaoTableA1.xls>). Figure 11 illustrates variation of initial ϵ_{Hf} with time, while figure 12 shows distribution of T_{DM2} model ages. There are eight zircons from KH84 whose ϵ_{Hf} (t) is nearly chondritic (2.90 to -1.0). The values of other zircons of the two samples are < -1 . They show a clear decreasing trend with decreasing age and can be interpreted to have

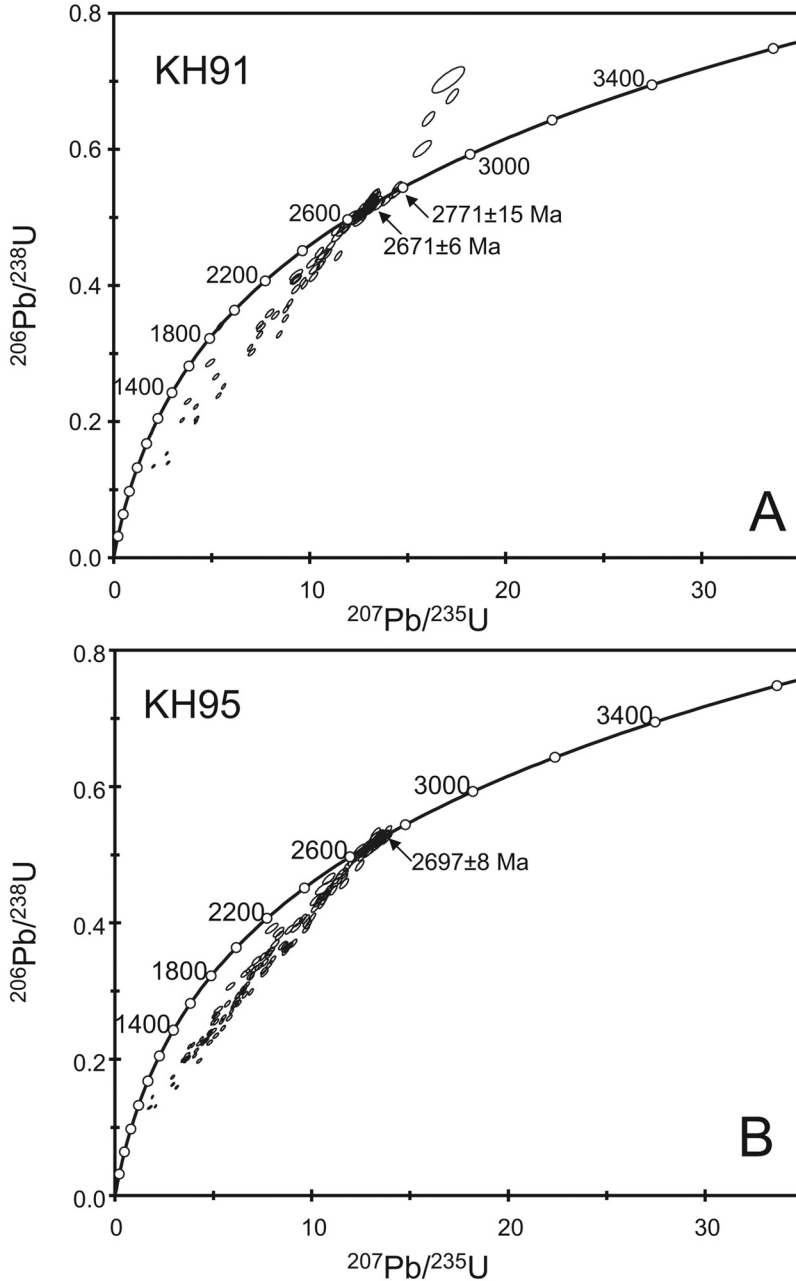


Fig. 10. Zircon U-Pb concordia plots for metasandstones KH91 (A) and KH95 (B) from the South Kongling terrain. Error ellipses are shown at 1 σ .

derived from 3.2 to 4.0 Ga old crustal source rocks at varying times (fig. 11A). Depleted mantle and crustal model ages of zircons with Th/U > 0.30 vary from 3.2 to 3.7 Ga and 3.2 to 3.9 Ga, respectively (Appendix table A1, <http://earth.geology.yale.edu/~ajs/SupplementaryData/2011/02GaoTableA1.xls>; fig. 12A).

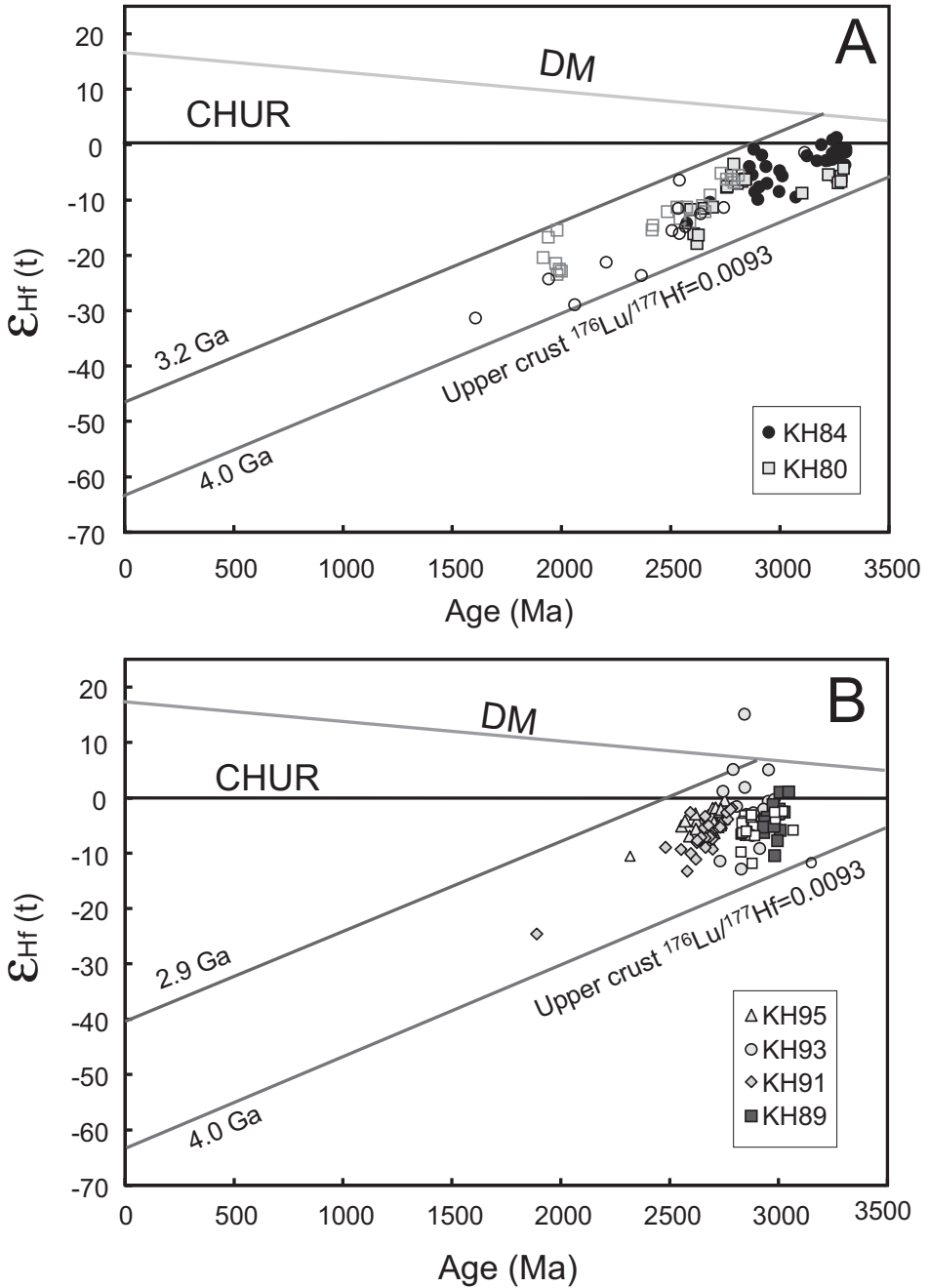


Fig. 11. Variation of Hf isotopes of zircons with age for rocks from the North Kongling terrain (A) and South Kongling terrain (B). Filled and open symbols indicate zircons with $\text{Th}/\text{U} \geq 3.0$ and < 3.0 , respectively. Also shown are evolution trends of depleted mantle (DM), chondritic reservoir (CHUR) and continental crust separated from the depleted mantle at 4.0 Ga, 3.2 Ga (A) and 2.9 Ga (b) with $^{176}\text{Lu}/^{177}\text{Hf} = 0.0093$ (Vervoort and Patchett, 1996).

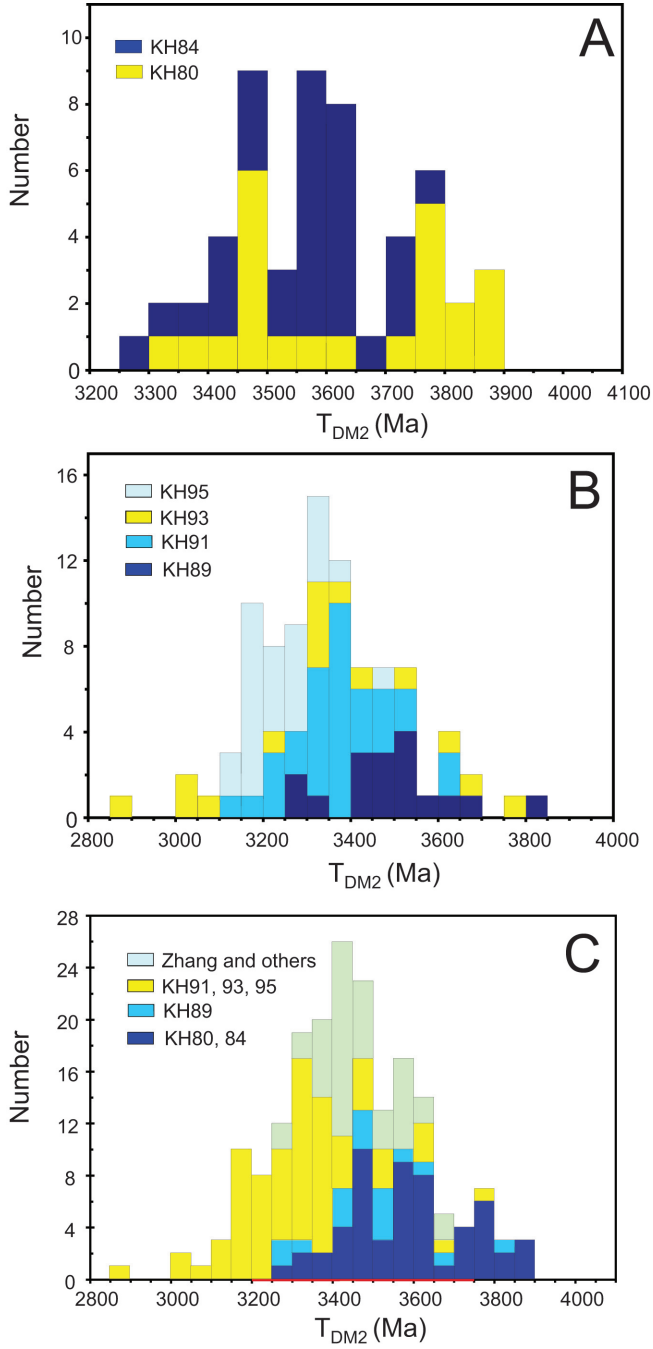


Fig. 12. Distribution of two-stage Hf model ages (T_{DM2}) of zircons with $Th/U \geq 0.30$ for rocks from the North Kongling terrain (A), the South Kongling terrain (B) and all available data for the Kongling terrain (C), which are grouped into the North Kongling granitoid gneisses (KH80 and KH84), South Kongling granitoid gneiss (KH89) and South Kongling metasedimentary rocks (KH91, KH93 and KH95). For comparison also shown in panel (C) are data for three ~ 2.9 Ga granitoid gneisses of the North Kongling terrain reported by Zhang and others (2006b).

South Kongling Terrain

35, 33, 17, and 28 concordant zircons from KH89, KH91, KH93 and KH95 were analyzed for Hf isotopes, respectively (Appendix table A1, <http://earth.geology.yale.edu/~ajs/SupplementaryData/2011/02GaoTableA1.xls>). As shown in figure 11B and Appendix table A1, <http://earth.geology.yale.edu/~ajs/SupplementaryData/2011/02GaoTableA1.xls>, there are four 2.7 to 2.9 Ga zircons from KH93 that have $\epsilon_{\text{Hf}}(t) = 1.1$ to 5.1. One zircon [KH93-26 (2844 Ma)] has $\epsilon_{\text{Hf}}(t) = 15$, which is significantly above the coeval depleted mantle value, the reason for which is unclear. Two grains from KH89 (KH89-25 and KH89-57) also have $\epsilon_{\text{Hf}}(t)$ close to 1.0. All other zircons from the South Kongling have negative $\epsilon_{\text{Hf}}(t)$. They can be interpreted to have derived from 2.9 to 4.0 Ga old crustal source rocks at varying times (fig. 11B). Their depleted mantle and crustal model ages vary from 2.9 to 3.6 Ga and 2.9 to 3.8 Ga, respectively (excluding KH93-26) (Appendix table A1, <http://earth.geology.yale.edu/~ajs/SupplementaryData/2011/02GaoTableA1.xls>; fig. 12B).

DISCUSSION

3.3 Ga Granitoid Magmatism

The following four lines of evidence show that the 3.2 to 3.3 Ga zircons in KH84 from the eastern segment of the North Kongling terrain represent age of the crystallization of the trondhjemite magma. First, these zircons are prismatic and show no age zoning and later overgrowth except for very thin bright rims on some of them (figs. 4F to 4L). This is unlike the xenocryst zircons that all occur as absorbed cores overgrown by younger 2.8 to 2.9 Ga zircons (Zhang and others, 2006b). Second, they form the major concordant age population, which contrasts with the scarcity of their inherited counterparts (Zhang and others, 2006b). Third, they exhibit clear oscillatory zoning and Th/U ratio ranging from 0.18 to 0.77, features typical of magmatic zircons (Hoskin and Schaltegger, 2003). Finally, as described above, unlike KH80, the outcrop for KH84 is relatively homogeneous and injection of migmatic veins is invisible (fig. 2B).

The 3.2 to 3.3 Ga zircon cores in KH80 may be interpreted in two ways. In the first scenario, they were inherited and entrained from the nearby trondhjemite like KH84. Thus, the granodiorite magma crystallized at 2.8 Ga. Alternatively, the granitoid magma crystallized at 3.3 Ga and the 2.8 Ga zircons represent later overgrowth. Compared to KH84, the outcrop of KH80 is heterogeneous and migmatized (fig. 2A) and contains more K-feldspar and higher K_2O , indicating more extensive later alteration and overprinting. This is supported by the apparently complicated age patterns of KH80 compared to KH84. For example, few zircons from KH84 have apparent $^{207}\text{Pb}/^{206}\text{Pb}$ ages younger than 1800 Ma. This is in great contrast to the KH80, which experienced significant lead loss at ~ 600 Ma (fig. 5A).

Nevertheless, KH84 is 3.2 to 3.3 Ga trondhjemite. Its best estimate of emplacement age is represented by the two oldest concordant analyses (KH84-6C and KH84-18C), which give identical $^{206}\text{Pb}/^{207}\text{Pb}$ age of $3302 \pm 7/8$ Ma (Appendix table A1, <http://earth.geology.yale.edu/~ajs/SupplementaryData/2011/02GaoTableA1.xls>). As evidenced by cathodoluminescence imaging, Th/U ratios (fig. 7A) and discordia defined by *in-situ* analyses (fig. 5B), the younger zircons from the same group resulted from variable late disturbance. Thus, the trondhjemitic gneisses represent the oldest known rocks in South China. Regardless as inherited or not, the zircon cores of similar ages in KH80 crystallized from a magma indistinguishable in age with the trondhjemite.

Multiple Zircon Overgrowths

The major younger zircon populations occur at 2.8 to 2.9 Ga, 2.5 to 2.6 Ga, and 1.9 to 2.2 Ga. Of them the 2.8 to 2.9 Ga igneous zircons were well documented by DTTG gneisses in the western segment of the North Kongling terrain (Gao and others, 1999;

Qiu and others, 2000; Zhang and others, 2006b). They show oscillatory zoning with Th/U ratios being 0.26 to 1.12. They represent magmatism which produced rocks dominating the Kongling terrain. The 2.5 to 2.6 Ga magmatism is unknown in the Kongling terrain (Gao and others, 1999; Qiu and others, 2000; Zhang and others, 2006b; Jiao and others, 2009). They exhibit weak oscillatory zoning and sometimes occur as core (KH84-34C) within older (2.8 Ga) mantle (KH84-34R1) (fig. 4N). Their Th/U ratios are low and range from 0.05 to 0.36. These lines of evidence suggest that they are most likely to be metamorphic. The 1.9 to 2.2 Ga zircons typically show patch structure (KH80-11) or are black structureless (KH84-26C) (figs. 4E and 4M). In the latter case, their rim (KH84-26R) is older (3008 Ma) (fig. 4M), implying recrystallization of the core during growth of the rim over it. This is consistent with their very low Th/U ratios (0.05-0.11) (Appendix table A1, <http://earth.geology.yale.edu/~ajs/SupplementaryData/2011/02GaoTableA1.xls>). Zircons of this age group were also found in DTTG gneisses from the western segment of the North Kongling terrain (Qiu and others, 2000; Zhang and others, 2006b). Ling and others (2001) obtained whole-rock-garnet-plagioclase Sm-Nd isochron ages of 1939 ± 44 Ma and 1958 ± 15 Ma from a paragneiss and an amphibolite in the North Kongling terrain, respectively. As described above, the K-feldspar-rich Quanqitang granite and mafic dikes, which intruded into the Kongling gneisses (fig. 1), yielded a U-Pb zircon age of 1854 ± 17 Ma (2σ) (Xiong and others, 2009) and 1852 ± 11 Ma (2σ) (Peng and others, 2009), respectively. These observations point out that the 1.9 to 2.2 Ga zircons reflect an important tectono-thermal and metamorphic event that led to the amphibolite-granulite-facies metamorphism of the Kongling terrain and produced the Quanqitang granite. The concordant 1.6 Ga zircon (KH84-20) shows very weak zoning (fig. 4O) and also has very low Th/U ratio of 0.04 and is thus likely to be metamorphic as well.

As described above, for the North Kongling gneisses KH80 and KH84 all the >2.8 Ga zircons show oscillatory zoning and have Th/U that varies from 0.30 up to 1.2, typical of igneous zircons, whereas <2.4 Ga zircons are typically structureless and have a lower Th/U ratio (0.20 to 0.04; fig. 7A), characteristic of metamorphic zircons (Hoskin and Schaltegger, 2003). Zircons of the intermediate ages (2.4-2.8 Ga) show intermediate Th/U ratios (0.2-0.4). These features indicate that the <2.4 Ga zircons are metamorphic and the >2.8 Ga zircons are mainly igneous.

The Pb loss at 600 to 730 Ma is apparent from the lower intercept for both granodioritic gneisses KH80 and KH89 from North and South Kongling (figs. 5 and 8). Most of zircons from the three metasedimentary samples from the South Kongling terrain also define discordias with lower intercepts also at 600 to 730 Ma (figs. 8 and 10). They suggest that the metasediments were derived mainly from single sources and that their zircons were also subjected to Pb loss at 600 to 730 Ma. The age of Pb loss is broadly correlative to the extensive magmatism of the Huanglin intrusive complex at 750 to 820 Ma, as described above. Magmatism of similar ages is widespread in South China and is considered to be related to the breakup of the Rodinian supercontinent (Li and others, 1999, 2006 and references therein). Unfortunately, the precise age of the Pb loss is poorly constrained with a large error (120 Ma) for the lower intercept (fig. 8A), and only one ~ 600 Ma zircon for KH80.

Correlation of the South and North Kongling Terrains

As described above, concordant zircons at the upper intercept of granodioritic gneiss KH89 from the South Kongling terrain give a weighted average $^{206}\text{Pb}/^{207}\text{Pb}$ age of 2981 ± 13 Ma, which is indistinguishable from the upper intercept age of 2951 ± 20 Ma within error. Together with their high Th/U ratios (0.20-1.55) and oscillatory zoning, 2981 Ma is interpreted to represent the age of the granodiorite magmatism. The significantly low Th/U ratios (0.08-0.20) and structureless CL images (figs. 9D and 9E) of the younger 2.8 Ga zircons indicate metamorphic overgrowth. The age of the

granodioritic gneiss is similar to those of the trondhjemitic and migmitic gneisses from the western segment of the North Kongling terrain (2903-2947 Ma) (Qiu and others, 2000; Zhang and others, 2006b). A similar magmatic age group (2913 ± 18 Ma) is also recorded in KH84 from the eastern segment of the North Kongling terrain. Zircon initial ϵ_{Hf} at 2.9 Ga for KH89 range from 1.07 to -10.5 with an average of -4.0 ± 2.9 (1σ). Their T_{DM2} ages vary from 3.3 to 3.7 Ga with an average of 3.49 ± 0.13 Ga (1σ). The Hf isotopic compositions are similar to those of 2.9 Ga zircons in three granitoid gneisses from the North Kongling terrain (Zhang and others, 2006b), which have initial ϵ_{Hf} in the range from 0 to -8.6 with an average of -4.0 ± 2.0 (1σ) and T_{DM2} in the range from 3.3 to 3.7 Ga with an average of 3.45 ± 0.10 Ga (2σ). They are also similar to the 2.9 Ga zircons from KH80 and KH84, which have initial ϵ_{Hf} in the range from -1.9 to -8.5 with an average of -5.6 ± 2.5 (1σ) and T_{DM2} in the range from 3.3 to 3.7 Ga with an average of 3.54 ± 0.13 Ga (2σ). It is therefore concluded that the South Kongling terrain correlates with its northern counterpart. The 2.9 Ga granitoid magmatism dominates the entire Kongling terrain. Whether 3.3 Ga granitoid magmatism existed in the South Kongling terrain needs further studies.

Hf Isotope Behavior During Metamorphism

CL images and Th/U ratios suggest that for the North Kongling granitoid gneisses KH80 and KH84, the <2.4 Ga zircons are metamorphic, whereas the >2.8 Ga ones are igneous. Figure 11A shows that although the post-Archean zircons from these two samples evolved to lower ϵ_{Hf} (t), all the zircons, regardless of their age, can be interpreted by being derived from crustal sources formed between 3.2 and 4.0 Ga. Concordant zircons in granodioritic gneiss KH89 from the South Kongling terrain formed in a relative narrow age range (2827 to 3066 Ma). Their ϵ_{Hf} (t) does not change with the highly variable Th/U ratio (0.05 to 1.55) (fig. 7B; Appendix table A1, <http://earth.geology.yale.edu/~ajs/SupplementaryData/2011/02GaoTableA1.xls>); zircons with Th/U < 3.0 have ϵ_{Hf} (t) values similar to those with Th/U > 3.0 (fig. 11B). It is thus suggested that the Lu-Hf isotopes in the three amphibolite-facies granitoid gneisses were largely immune to later metamorphism. The general immobility of Hf isotopes during metamorphic processes was also inferred from previous studies (Schmidberger and others, 2005; Zheng and others, 2006; Wu and others, 2007). The relatively large spread in ϵ_{Hf} (t) of the three granitoid gneisses (fig. 11) at a given age may be attributed to source heterogeneities or mixing between mantle-derived and crustal magmas.

Source Provenance of Metasediments

All three metasedimentary rocks from the South Kongling terrain show prominent negative Eu anomalies ($\text{Eu}/\text{Eu}^* = 0.53-0.75$), which are similar to those of post-Archean shales (Taylor and McLennan, 1985; Rudnick and Gao, 2003). Except four >3.0 Ga zircons, detrital zircons from these three clastic metasediments define discordias with upper intercept ages of 2.9 Ga for metapelites KH93 and 2.6 Ga for metasandstones KH91 and KH95. The lower intercepts are anchored at 600 to 730 Ma, which is similar to the age of widespread Neoproterozoic Huangling magmatism to the south. Accordingly the discordias represent varying Pb loss of the Archean zircons due to the Neoproterozoic magmatism. This indicates that the three South Kongling metasediments were derived from single sources of similar ages. Since Archean rocks of varying ages are present in the Kongling terrain and the age variability is not observed in metasandstones KH91 and KH95, this further implies that these two samples were derived from a near source. The concordant age group of KH93 agrees with those of DTTG gneisses from the western segment of the North Kongling terrain and the South Kongling terrain, and can be interpreted to have been derived from these DTTG gneisses. Three *ca.* 3.2 Ga zircons can also be interpreted similarly as

inherited zircons or being derived from the trondhjemitic in the eastern segment of the North Kongling terrain. However, the source of the 3.4 Ga zircon is unknown in the Kongling terrain and needs further study.

The three metasediments from the South Kongling terrain display coupled Eu and Sr depletions (figs. 3A and 3B). These features contrast with the absence of Eu and Sr depletions in the 2.9 Ga DTTG gneisses, which are characterized by variable Sr enrichments. Because Sr and Eu are predominantly hosted by plagioclase, the above observations indicate that the development of negative Sr and Eu depletions in the South Kongling metasediments is due to preferential decomposition of plagioclase in the source rocks. These results reinforced that the Eu depletion of the clastic sedimentary rocks are largely controlled by decomposition of plagioclase (Gao and Wedepohl, 1995).

Crustal Growth

The Kongling terrain contains the only known exposed Archean rocks of the Yangtze craton (Gao and Zhang, 1990; Gao and others, 1999; Qiu and others, 2000; Zhang and others, 2006b; Jiao and others, 2009). According to this study and previous works (Qiu and others, 2000; Zhang and others, 2006b; Jiao and others, 2009), trondhjemitic and migmatitic gneisses from the western segment of the North Kongling terrain and the South Kongling terrain are 2.90 to 2.95 Ga in age, while they are apparently older (3.2–3.3 Ga) in the eastern segment of the North Kongling terrain. Detrital zircons from the Kongling metapelites are 2.87 to 3.28 Ga in age (Qiu and others, 2000). Few ≥ 3.5 Ga zircons as well as 3.6 to 4.0 Ga Hf model ages obtained by previous studies (Liu and others, 2006, 2008; Zhang and others, 2006a) and this study documents the existence of Eoarchean crust. The tonalitic, trondhjemitic and granitic gneisses, amphibolites and metasedimentary rocks (excluding resitite components of high grade metasedimentary rocks, whose Sm-Nd isotopic compositions were disturbed) have Nd model ages in the range of 2.7 to 4.2 Ga (Gao and others, 1999). As discussed above and shown by Zhang and others (2006a), abundant zircons show Hf model ages of a similar range. Taken together, previous data suggest that there are several episodes of Archean crustal growth in the Yangtze craton with four age peaks at 2.35 to 2.50 Ga, 2.60 to 2.70 Ga, 2.95 to 3.00 Ga and 3.20 to 3.80 Ga (Zhang and others, 2006a; Liu and others, 2008).

Since most of our dated zircons have $\epsilon_{\text{Hf}}(t) \leq 0$, indicating that they were derived from the pre-existing 2.9 to 4.0 Ga continental crust. For such zircons the two-stage Hf model ages may better indicate the separation age of their crustal source from the mantle, that is, the crustal formation age (fig. 12). The two granodioritic and trondhjemitic gneisses from the North Kongling terrain have $T_{\text{DM}2}$ in the range from 3.2 and 3.9 Ga with an average of 3.69 ± 0.30 (2σ) (fig. 12A). The granodioritic gneiss from the South Kongling terrain shows a similar $T_{\text{DM}2}$ range but the average [3.49 ± 0.26 (2σ)] is apparently younger (fig. 12B). The $T_{\text{DM}2}$ of the three metasedimentary rocks from the South Kongling terrain are significantly younger in the range (2.85–3.80 Ga) and the average [3.32 ± 0.30 (2σ)] (fig. 12B). Together with results for three ~ 2.9 Ga granitoid gneisses from the North Kongling terrain (Zhang and others, 2006b), all the available 180 zircon Hf analyses from the Kongling terrain show a major $T_{\text{DM}2}$ range between 3.15 and 3.8 Ga and a significant peak at 3.3 to 3.5 Ga with an average of 3.41 ± 0.80 (2σ) (fig. 12C).

The two granodioritic and trondhjemitic gneisses from the North Kongling terrain have identical Nd model ages of 3.4 Ga, close to their oldest age of magmatism and consistent with the Hf model age peak. Their ϵ_{Nd} values at 3.3 Ga are nearly chondritic (0.24–1.26). Together with some of zircons from KH84 that have nearly chondritic $\epsilon_{\text{Hf}}(t)$, the above lines of evidence suggest that the 3.3 Ga granitoids represent juvenile crust additions to the pre-existing continental crust.

Our results contrast with combined zircon age and Nd isotopic studies of worldwide granitoids (Condie and others, 2009), which show that granitoid episodes that are clearly important times of juvenile continental crust production occur at 2700, 2550, 2120, 1900, 1700, 1650, 800, 570 and 450 Ma. The results also contrast with studies of detrital zircons from the Yellow River and two smaller rivers from North China, which suggest significant peaks of crust formation at 2.7 to 2.8 Ga (Yang and others, 2009). However, our results agree with Hf isotope data for detrital zircons from eastern Australia, which suggest a major pulse of Archean juvenile crust production in part of Gondwana at 3.3 Ga (Kemp and others, 2006). It is apparent that crustal growth history show significant regional variations. Therefore, the construction of the global crustal growth history has to be based upon data from as large as possible areas. In addition, the present results reinforce our previous studies (Gao and others, 2004; Liu and others, 2008) that North China and South China have distinct histories of crustal formation and evolution.

CONCLUSIONS

The igneous protolith of trondhjemitic gneisses from the North Kongling terrain crystallized at 3302 Ma. It represents the oldest known rock component in South China and predates the previously reported ~ 2.9 Ga granitoid magmatism by 400 Ma.

Igneous zircons in one granodioritic gneiss from the South Kongling terrain yield a weighted mean $^{206}\text{Pb}/^{207}\text{Pb}$ age of 2981 ± 13 Ma. The zircon age and initial Hf isotopic compositions are similar to those of the granitoid gneisses from the North Kongling, and indicates that the South and North Kongling terrains are correlative. Our results also reinforce that magmatism of the whole Kongling terrain mainly occurred at 2.9 Ga.

Available Hf isotopic data from the Kongling terrain show that juvenile crustal additions occurred mainly between 3.15 and 3.8 Ga with a significant peak at 3.3 to 3.5 Ga. This is well exemplified by the 3.3 Ga trondhjemitic gneiss which has a Nd model age of 3.4 Ga with a nearly chondritic ϵ_{Nd} value at 3.3 Ga and some of whose zircons have nearly chondritic ϵ_{Hf} (t).

Our results contrast with combined zircon age and Nd isotopic studies of worldwide granitoids, which show that granitoid episodes that are clearly important times of Archean juvenile continental crust production occur at 2700 and 2550 Ma. The results also contrast with studies of detrital zircons from the Yellow River and two smaller rivers from North China, which suggest a significant peak of crust formation at 2.7 to 2.8 Ga. However, our results agree with Hf isotope data for detrital zircons from eastern Australia, which suggest a major pulse of Archean juvenile crust production in part of Gondwana at 3.3 Ga. It is apparent that crustal growth history show significant regional variations. Therefore, the construction of the global crustal growth history has to be based upon data from as large as possible areas. In addition, the present results reinforce our previous studies that North China and South China have distinct histories of crustal formation and evolution.

ACKNOWLEDGMENTS

This research was supported by the National Nature Science Foundation of China (40973020, 91014007, 90714010, 40821061), Chinese Ministry of Education (B07039), the MOST special funds from the State Key Laboratory of Continental Dynamics and the State Key Laboratory of Geological Processes and Mineral Resources, the Fok Ying Tong Education Foundation (121017), and the Fundamental Research Funds for the Central Universities (CUGL100401 and CUG090105). We thank Jianxiong Wang for help in the field work. We also thank W. L. Ling, Y. Liu and J. Q. Wang for analyzing the whole-rock chemical and isotopic compositions. We finally thank John Ayers, Kent

Condie, Randall Parrish and two anonymous reviewers for their comments, which helped to improve the manuscript significantly.

APPENDIX

TABLE A1

<http://earth.geology.yale.edu/~ajs/SupplementaryData/2011/02GaoTableA1.xls>

TABLE A2

<http://earth.geology.yale.edu/~ajs/SupplementaryData/2011/03GaoTableA2.xls>

REFERENCES

- Andersen, T., 2002, Correction of common lead in U-Pb analyses that do not report ^{204}Pb : *Chemical Geology*, v. 192, p. 59–79, doi:10.1016/S0009-2541(02)00195-X.
- Ayers, J. C., Dunkle, S., Gao, S., and Miller, C. F., 2002, Constraints on timing of peak and retrograde metamorphism in the Dabie Shan Ultrahigh-Pressure Metamorphic Belt, east-central China, using U-Th-Pb dating of zircon and monazite: *Chemical Geology*, v. 186, p. 315–331, doi:10.1016/S0009-2541(02)00008-6.
- Bichert-Toft, J., and Albarède, F., 1997, The Lu-Hf isotope geochemistry of chondrites and the evolution of the mantle-crust system: *Earth and Planetary Science Letters*, v. 148, p. 243–258, doi:10.1016/S0012-821X(97)00040-X.
- Chu, N. C., Taylor, R. N., Chavagnac, V., Nesbitt, R. W., Boella, R. M., Milton, J. A., German, C. R., Bayon, G., and Burton, K., 2002, Hf isotope ratio analysis using multi-collector inductively coupled plasma mass spectrometry: an evaluation of isobaric interference corrections: *Journal of Analytical Atomic Spectrometry*, v. 17, p. 1567–1574, doi:10.1039/b206707b.
- Condie, K. C., 1998, Episodic continental growth and supercontinents: a mantle avalanche connection: *Earth and Planetary Science Letters*, v. 163, p. 97–108, doi:10.1016/S0012-821X(98)00178-2.
- 2000, Episodic continental growth models: afterthoughts and extensions: *Tectonophysics*, v. 322, p. 153–162, doi:10.1016/S0040-1951(00)00061-5.
- Condie, K. C., Beyer, E., Belousova, E. A., Griffin, W. L., and O'Reilly, S. Y., 2005, U-Pb isotopic ages and Hf isotopic composition of single zircons: The search for juvenile Precambrian continental crust: *Precambrian Research*, v. 139, p. 42–100, doi:10.1016/j.precamres.2005.04.006.
- Condie, K. C., Belousova, E. A., Griffin, W. L., and Sircombe, K. N., 2009, Granitoid events in space and time: Constraints from igneous and detrital zircon age spectra: *Gondwana Research*, v. 15, p. 228–242, doi:10.1016/j.gr.2008.06.001.
- De Bievre, P., and Taylor, P. D. P., 1993, Table of the isotopic compositions of the elements: *International Journal of Mass Spectrometry and Ion Processes*, v. 123, p. 149–166, doi:10.1016/0168-1176(93)87009-H.
- DePaolo, D. J., and Wasserburg, G. J., 1976, Inferences about magma sources and mantle structure from variations of $^{143}\text{Nd}/^{144}\text{Nd}$: *Geophysical Research Letters*, v. 3, p. 743–746, doi:10.1029/GL003i012p00743.
- Eggins, S. M., Kinsley, L. P. J., and Shelley, J. M. G., 1998, Deposition and element fractionation processes during atmospheric pressure laser sampling for analysis by ICP-MS: *Applied Surface Science*, v. 127/129, p. 278–286, doi:10.1016/S0169-4332(97)00643-0.
- Gao, S., and Wedepohl, K. H., 1995, The negative Eu anomaly in Archean sedimentary rocks: Implications for decomposition, age and importance of their granitic sources: *Earth and Planetary Science Letters*, v. 133, p. 81–94, doi:10.1016/0012-821X(95)00077-P.
- Gao, S., and Zhang, B.-R., 1990, The discovery of Archean TTG gneisses in northern Yangtze craton and their implications: *Earth Science*, v. 15, p. 675–679 (in Chinese with English abstract).
- Gao, S., Ling, W. L., Qiu, Y., Zhou, L., Hartmann, G., and Simon, K., 1999, Contrasting geochemical and Sm-Nd isotopic compositions of Archean metasediments from the Kongling high-grade terrain of the Yangtze craton: Evidence for cratonic evolution and redistribution of REE during crustal anatexis: *Geochimica et Cosmochimica Acta*, v. 63, p. 2071–2088, doi:10.1016/S0016-7037(99)00153-2.
- Gao, S., Rudnick, R. L., Yuan, H. L., Liu, X. M., Liu, Y. S., Xu, W. L., Ling, W. L., Ayers, J. C., Wang, X. C., and Wang, Q. H., 2004, Recycling lower continental crust in the North China craton: *Nature*, v. 432, p. 892–897, doi:10.1038/nature03162.
- Griffin, W. L., Pearson, N. J., Belousova, E., Jackson, S. E., Achterbergh, E. V., O'Reilly, S. Y., and Shee, S. R., 2000, The Hf isotope composition of cratonic mantle: LAM-MC-ICPMS analysis of zircon megacrysts in kimberlites: *Geochimica et Cosmochimica Acta*, v. 64, p. 133–147, doi:10.1016/S0016-7037(99)00343-9.
- Hacker, B. R., Ratschbacher, L., Webb, L., Ireland, T., Walker, D., and Dong, S., 1998, U/Pb zircon ages constrain the architecture of the ultrahigh-pressure Qinling-Dabie Orogen, China: *Earth and Planetary Science Letters*, v. 161, p. 215–230, doi:10.1016/S0012-821X(98)00152-6.
- Hawkesworth, C. J., and Kemp, A. I. S., 2006a, Evolution of the continental crust: *Nature*, v. 443, p. 811–817, doi:10.1038/nature05191.
- 2006b, Using hafnium and oxygen isotopes in zircons to unravel the record of crustal evolution: *Chemical Geology*, v. 226, p. 144–162, doi:10.1016/j.chemgeo.2005.09.018.

- Hoskin, P. W. O., and Schaltegger, U., 2003, The composition of zircon and igneous and metamorphic petrogenesis, *in* Hanchar, J. M., and Hoskin, P. W. O., editors, *Zircon: Mineralogical Society of America, Reviews in Mineralogy and Geochemistry*, v. 53, p. 27–62, doi:10.2113/0530027.
- Iizuka, T., and Hirata, T., 2005, Improvements of precision and accuracy in *in-situ* Hf isotope microanalysis of zircon using the laser ablation-MC-ICPMS technique: *Chemical Geology*, v. 220, p. 121–137, doi:10.1016/j.chemgeo.2005.03.010.
- Iizuka, T., Hirata, T., Komiya, T., Rino, S., Katayama, I., Motoki, A., and Maruyama, S., 2005, U-Pb and Lu-Hf isotopic systematics of zircons from the Mississippi River sand: Implications for reworking and growth of continental crust: *Geology*, v. 33, p. 485–488, doi:10.1130/G21427.1.
- Jackson, S. E., Pearson, N. J., Griffin, W. L., and Belousova, E. A., 2004, The application of laser ablation–inductively coupled plasma–mass spectrometry to *in situ* U-Pb zircon geochronology: *Chemical Geology*, v. 211, p. 47–69, doi:10.1016/j.chemgeo.2004.06.017.
- Jiao, W. F., Wu, Y. B., Yang, S. H., Peng, M., and Wang, J., 2009, The oldest basement rock in the Yangtze Craton revealed by zircon U-Pb age and Hf isotope composition: *Science in China Series D*, v. 52, p. 1393–1399, doi:10.1007/s11430-009-0135-7.
- Kemp, A. I. S., Hawkesworth, C. J., Paterson, B. A., and Kinny, P. D., 2006, Episodic growth of the Gondwana supercontinent from hafnium and oxygen isotopes in zircon: *Nature*, v. 439, p. 580–583, doi:10.1038/nature04505.
- Li, X. H., Li, Z. X., Sinclair, J. A., Li, W. X., and Carter, G., 2006, Revisiting the “Yanbian Terrane”: Implications for Neoproterozoic tectonic evolution of the western Yangtze Block, South China: *Precambrian Research*, v. 151, p. 14–30, doi:10.1016/j.precamres.2006.07.009.
- Li, Z. X., Li, X. H., Kinny, P. D., and Wang, J., 1999, The breakup of Rodinia: did it start with a mantle plume beneath South China?: *Earth and Planetary Science Letters*, v. 173, p. 171–181, doi:10.1016/S0012-821X(99)00240-X.
- Ling, W. L., Gao, S., Cheng, J. P., Jiang, L. S., Yuan, H. L., and Hu, Z. C., 2006, Neoproterozoic magmatic events within the Yangtze continental interior and along its northern margin and their tectonic implication: Constraint from the ELA-ICP-MS U-Pb geochronology of zircons from the Huangling and Hannan complexes: *Acta Petrologica Sinica*, v. 22, p. 387–396 (in Chinese with English abstract).
- Liu, X. M., Gao, S., Ling, W. L., Yuan, H. L., and Hu, Z. C., 2006, Identification of 3.5 Ga detrital zircons from Yangtze craton in south China and the implication for Archean crust evolution: *Progress in Natural Science*, v. 16, p. 663–666, doi:10.1080/10020070612330050.
- Liu, X. M., Gao, S., Diwu, C. R., and Ling, W. L., 2008, Precambrian crustal growth of Yangtze Craton as revealed by detrital zircon studies: *American Journal of Science*, v. 308, p. 421–468, doi:10.2475/04.2008.02.
- Ludwig, K. R., 2003, *ISOPLOT 3: A Geochronological Toolkit for Microsoft Excel*: Berkeley Geochronology Centre Special Publication 4, 74 p.
- Ma, G., Lee, H., and Zhang, Z., 1984, An investigation of the age limits of the Sinian System in South China: *Bulletin of Yichang Institute of Geology and Mineral Resources*, v. 8, p. 1–29 (in Chinese with English abstract).
- McDonough, W. F., and Sun, S.-S., 1995, The composition of the Earth: *Chemical Geology*, v. 120, p. 223–253, doi:10.1016/0009-2541(94)00140-4.
- Peng, M., Wu, Y. B., Wang, J., Jiao, W. F., Liu, X. C., and Yang, S. H., 2009, Paleoproterozoic mafic dyke from Kongling terrain in the Yangtze Craton and its implication: *Chinese Science Bulletin*, v. 54, p. 1098–1104, doi:10.1007/s11434-008-0558-0.
- Qiu, Y. M., Gao, S., McNaughton, N. J., Groves, D. I., and Ling, W. L., 2000, First evidence of >3.2 Ga continental crust in the Yangtze craton of south China and its implications for Archean crustal evolution and Phanerozoic tectonics: *Geology*, v. 28, p. 11–14, doi:10.1130/0091-7613(2000)028(0011: FEOGCC)2.0.CO;2.
- Rudnick, R. L., and Gao, S., 2003, Composition of the continental crust, *in* Rudnick, R. L., editor, *The Crust: Treatise on Geochemistry*, v. 3, p. 1–64, doi:10.1016/B0-08-043751-6/03016-4.
- Rudnick, R. L., Gao, S., Ling, W. L., Liu, Y. S., and McDonough, W. F., 2004, Petrology and geochemistry of spinel peridotite xenoliths from Hannuoba and Qixia, North China craton: *Lithos*, v. 77, p. 609–637, doi:10.1016/j.lithos.2004.03.033.
- Scherer, E., Munker, C., and Mezger, K., 2001, Calibration of the lutetium-hafnium clock: *Science*, v. 293, p. 683–687, doi:10.1126/science.1061372.
- Schmidberger, S. S., Heaman, L. M., Simonetti, A., Creaser, R. A., and Cookenboo, H. O., 2005, Formation of Paleoproterozoic eclogitic mantle, Slave Province (Canada): Insights from *in-situ* Hf and U-Pb isotopic analyses of mantle zircons: *Earth and Planetary Science Letters*, v. 240, p. 621–633, doi:10.1016/j.epsl.2005.09.057.
- Taylor, S. R., and McLennan, S. M., 1985, *The Continental Crust: Its Composition and Evolution*: Oxford, Blackwell Scientific Publication, 311 p.
- Vermeesch, P., 2004, How many grains are needed for a provenance study?: *Earth and Planetary Science Letters*, v. 224, p. 441–451, doi:10.1016/j.epsl.2004.05.037.
- Vervoort, J. D., and Patchett, P. J., 1996, Behavior of hafnium and neodymium isotopes in the crust: Constraints from Precambrian crustally derived granites: *Geochimica et Cosmochimica Acta*, v. 60, p. 3717–3733, doi:10.1016/0016-7037(96)00201-3.
- Wiedenbeck, M., Allé, P., Corfu, F., Griffin, W. L., Meier, M., Oberli, F., Von Quadt, A., Roddick, J. C., and Spiegel, W., 1995, Three natural zircon standards for U-Th-Pb, Lu-Hf, trace-element and REE analyses: *Geostandards Newsletter*, v. 19, p. 1–23, doi:10.1111/j.1751-908X.1995.tb00147.x.
- Woodhead, J., Hergt, J., Shelley, M., Eggins, S., and Kemp, R., 2004, Zircon Hf-isotope analysis with an excimer laser, depth profiling, ablation of complex geometries, and concomitant age estimation: *Chemical Geology*, v. 209, p. 121–135, doi:10.1016/j.chemgeo.2004.04.026.

- Wu, Y.-B., Zheng, Y.-F., Zhang, S.-B., Zhao, Z.-F., Wu, F.-Y., and Liu X.-M., 2007, Zircon U-Pb ages and Hf isotope compositions of migmatite from the North Dabie terrane in China: constraints on partial melting: *Journal of Metamorphic Geology*, v. 25, p. 991–1009, doi:10.1111/j.1525-1314.2007.00738.x.
- Xiong, Q., Zheng, J. P., Yu, C. M., Su, Y. P., Tang, H. Y., and Zhang, Z. H., 2009, Zircon U-Pb age and Hf isotope of Quanyishang A-type granite in Yichang: Signification for the Yangtze continental cratonization in Paleoproterozoic: *Chinese Science Bulletin*, v. 54, p. 436–446, doi:10.1007/s11434-008-0401-7.
- Yang, J., Gao, S., Chen, C., Tang, Y. Y., Yuan, H. L., Gong, H. J., Xie, S. W., and Wang, J. Q., 2009, Episodic crustal growth of North China as revealed by U-Pb age and Hf isotopes of detrital zircons from modern rivers: *Geochimica et Cosmochimica Acta*, v. 73, p. 2660–2673, doi:10.1016/j.gca.2009.02.007.
- Yuan, H. L., Gao, S., Liu, X. M., Li, H. M., Günther, D., and Wu, F. Y., 2004, Accurate U-Pb Age and Trace Element Determinations of Zircon by Laser Ablation-Inductively Coupled Plasma Mass Spectrometry: *Geostandards Newsletter*, v. 28, p. 353–370, doi:10.1111/j.1751-908X.2004.tb00755.x.
- Yuan, H. L., Gao, S., Dai, M. N., Zong, C. L., Günther, D., Fontaine, G. H., Liu, X. M., and Diwu, C. R., 2008, Simultaneous determinations of U-Pb age, Hf isotopes and trace element compositions of zircon by excimer laser-ablation quadrupole and multiple-collector ICP-MS: *Chemical Geology*, v. 247, p. 100–118, doi:10.1016/j.chemgeo.2007.10.003.
- Zhang, S. B., Zheng, Y. F., Wu, Y. B., Zhao, Z. F., Gao, S., and Wu, F. Y., 2006a, Zircon U-Pb age and Hf isotope evidence for 3.8 Ga crustal remnant and episodic reworking of Archean crust in South China: *Earth and Planetary Science Letters*, v. 252, p. 56–71, doi:10.1016/j.epsl.2006.09.027.
- 2006b, Zircon isotope evidence for ≥ 3.5 Ga continental crust in the Yangtze craton of China: *Precambrian Research*, v. 146, p. 16–34, doi:10.1016/j.precamres.2006.01.002.
- 2006c, Zircon U-Pb age and Hf-O isotope evidence for Paleoproterozoic metamorphic event in South China: *Precambrian Research*, v. 151, p. 265–288, doi:10.1016/j.precamres.2006.08.009.
- Zheng, J. P., Griffin, W. L., O'Reilly, S. Y., Zhang, M., Pearson, N., and Pan, Y., 2006, Widespread Archean basement beneath the Yangtze Craton: *Geology*, v. 34, p. 417–420, doi:10.1130/G22282.1.
- Zheng, Y. F., Fu, B., Gong, B., and Li, L., 2003, Stable isotope geochemistry of ultrahigh pressure metamorphic rocks from the Dabie-Sulu orogen in China: implications for geodynamics and fluid regime: *Earth Science Reviews*, v. 62, p. 105–161, doi:10.1016/S0012-8252(02)00133-2.
- Zheng, Y.-F., Zhao, Z.-F., Wu, Y.-B., Zhang, S.-B., Liu, X. M., and Wu F.-Y., 2006, Zircon U-Pb age, Hf and O isotope constraints on protolith origin of ultrahigh-pressure eclogite and gneiss in the Dabie orogen: *Chemical Geology*, v. 231, p. 135–158, doi:10.1016/j.chemgeo.2006.01.005.